19 Chang JW, Hsieh JJ, Shen YC *et al.* Bisphosphonate zoledronic acid enhances the inhibitory effects of gefitinib on EGFR-mutated non-small cell lung carcinoma cells. *Cancer Lett* 2009; **278**: 17–26.
20 Therasse P, Arbuck SG, Eisenhauer EA *et al.* New guidelines to evaluate the response to treatment in solid tumors. European Organization for Research and Treatment of Cancer, National Cancer Institute of the United States, National Cancer Institute of Canada. *J Natl Cancer Inst* 2000; **92**: 205–16.
21 Pandya KJ, Gajra A, Warsi GM *et al.* Multicenter, randomized, phase 2 study of zoledronic acid in combination with docetaxel and carboplatin in patients with unresectable stage IIIB or stage IV non-small cell lung cancer. *Lung Cancer* 2010; **67**: 330–8.
22 Scagliotti GV, Kosmidis P, de Marinis F *et al.* Zoledronic acid in patients with stage IIIA/B NSCLC: results of a randomized, phase III study. *Ann Oncol* 2012; **23**: 2082–7.
23 Henry DH, Costa L, Goldwasser F *et al.* Randomized, double-blind study of denosumab versus zoledronic acid in the treatment of bone metastases in patients with advanced cancer (excluding breast and prostate cancer) or multiple myeloma. *J Clin Oncol* 2011; **29**: 1125–32.
24 Scagliotti GV, Hirsh V, Siena S *et al.* Overall survival improvement in patients with lung cancer and bone metastases treated with denosumab versus zoledronic acid: subgroup analysis from a randomized phase 3 study. *J Thorac Oncol* 2012; **7**: 1823–9.
25 Hirsh V, Tchekmedyian NS, Rosen LS *et al.* Clinical benefit of zoledronic acid in patients with lung cancer and other solid tumors: analysis based on history of skeletal complications. *Clin Lung Cancer* 2004; **6**: 170–4.
26 Sekine I, Nokihara H, Yamamoto N *et al.* Risk factors for skeletal-related events in patients with non-small cell lung cancer treated by chemotherapy. *Lung Cancer* 2009; **65**: 219–22.
27 Brown JE, Cook RJ, Major P *et al.* Bone turnover markers as predictors of skeletal complications in prostate cancer, lung cancer, and other solid tumors. *J Natl Cancer Inst* 2005; **97**: 59–69.

Lung Cancer 84 (2014) 139–144

Contents lists available at ScienceDirect

Lung Cancer

journal homepage: www.elsevier.com/locate/lungcan

Molecular profiling of small cell lung cancer in a Japanese cohort

Kazushige Wakuda[a,b,*], Hirotsugu Kenmotsu[a,b], Masakuni Serizawa[b], Yasuhiro Koh[b], Mitsuhiro Isaka[c], Shoji Takahashi[c], Akira Ono[a], Tetsuhiko Taira[a], Tateaki Naito[a], Haruyasu Murakami[a], Keita Mori[d], Masahiro Endo[e], Takashi Nakajima[f], Yasuhisa Ohde[c], Toshiaki Takahashi[a], Nobuyuki Yamamoto[a,g]

[a] Division of Thoracic Oncology, Shizuoka Cancer Center, Nagaizumi-cho, Suntou-gun, Shizuoka, Japan
[b] Division of Drug Discovery and Development, Shizuoka Cancer Center Research Institute, Nagaizumi-cho, Suntou-gun, Shizuoka, Japan
[c] Division of Thoracic Surgery, Shizuoka Cancer Center, Nagaizumi-cho, Suntou-gun, Shizuoka, Japan
[d] Clinical Trial Coordination Office, Shizuoka Cancer Center, Nagaizumi-cho, Suntou-gun, Shizuoka, Japan
[e] Division of Diagnostic Radiology, Shizuoka Cancer Center, Nagaizumi-cho, Suntou-gun, Shizuoka, Japan
[f] Division of Pathology, Shizuoka Cancer Center, Nagaizumi-cho, Suntou-gun, Shizuoka, Japan
[g] Third Department of Internal Medicine, Wakayama Medical University, Kimiidera, Wakayama, Japan

ARTICLE INFO

Article history:
Received 18 November 2013
Received in revised form 5 February 2014
Accepted 23 February 2014

Keywords:
Small cell lung cancer
Molecular profiling
Genomic aberration
Driver mutation
PIK3CA
EGFR

ABSTRACT

Objectives: Advances in the molecular profiling of lung adenocarcinoma over the past decade have led to a paradigm shift in its diagnosis and treatment. However, there are very few reports on the molecular profiles of small cell lung cancers (SCLCs). We therefore conducted the present Shizuoka Lung Cancer Mutation Study to analyze genomic aberrations in patients with thoracic malignancies.
Materials and methods: We collected samples of SCLC from a biobank system and analyzed their molecular profiles. We assessed 23 mutations in nine genes (*EGFR, KRAS, BRAF, PIK3CA, NRAS, MEK1, AKT1, PTEN,* and *HER2*) using pyrosequencing plus capillary electrophoresis. We also amplified *EGFR, MET, PIK3CA, FGFR1,* and *FGFR2* using quantitative real-time polymerase chain reaction (PCR) and the fusion genes *ALK, ROS1,* and *RET* using reverse transcription PCR.
Results: Between July 2011 and January 2013, 60 SCLC patients were enrolled in the study. Samples included eight surgically resected snap-frozen samples, 50 formalin-fixed paraffin-embedded samples, and seven pleural effusion samples. We detected 13 genomic aberrations in nine cases (15%), including an *EGFR* mutation ($n=1$, G719A), a *KRAS* mutation ($n=1$, G12D), *PIK3CA* mutations ($n=3$, E542K, E545K, E545Q), an *AKT1* mutation ($n=1$, E17K), a *MET* amplification ($n=1$), and *PIK3CA* amplifications ($n=6$). *EGFR* and *KRAS* mutations were found in patients with combined SCLC and adenocarcinoma. No significant differences were detected in the characteristics of patients with and without genomic aberrations. However, serum neuron-specific enolase and progastrin-releasing peptide levels were significantly higher in patients without genomic aberrations than in those with aberrations ($p=0.01$ and 0.04, respectively).
Conclusion: Genomic aberrations were found in 15% SCLC patients, with *PIK3CA* amplifications most frequently observed. To further our understanding of the molecular profiles of SCLC, comprehensive mutational analyses should be conducted using massive parallel sequencing.

1. Introduction

Lung cancer is the most common cause of cancer-related deaths, and small cell lung cancer (SCLC) accounts for approximately 12% of all lung cancers [1]. It follows a very aggressive course, with approximately 60–70% patients having disseminated disease at diagnosis. Although SCLC shows high sensitivity to chemotherapy and radiotherapy, the median survival time for extended-disease SCLC is 8–13 months, and the 2-year survival rate is only 5% [2].

Molecular abnormalities have been discovered in patients with non-SCLC over the last decade, and these discoveries have led to a paradigm shift in its diagnosis and treatment. For example, a relationship between activating epidermal growth factor receptor (*EGFR*) mutations and response to gefitinib was reported in 2004 [3,4]. Subsequently, a number of randomized studies showed that patients with activating *EGFR* mutations were highly responsive to

* Corresponding author at: Division of Thoracic Oncology, Shizuoka Cancer Center Hospital, 1007 Shimonagakubo, Nagaizumi-cho, Suntou-gun, Shizuoka 411-8777, Japan. Tel.: +81 55 989 5222; fax: +81 55 989 5634.
E-mail address: h.kenmotsu@scchr.jp (K. Wakuda).

http://dx.doi.org/10.1016/j.lungcan.2014.02.013
0169-5002/

EGFR tyrosine kinase inhibitors such as gefitinib and erlotinib [5–8]. Currently, it is essential that lung adenocarcinomas are classified on the basis of genomic aberrations to ensure that patients are treated with the appropriate molecular-targeted drugs [9,10]. Analyses of genomic aberrations and the development of new molecular-targeted drugs are ongoing for lung adenocarcinoma. In contrast, there have been few innovations in the treatment of SCLC, despite extensive basic and clinical research over the past 30 years.

There have been few molecular profiles of SCLC, and, till date, no molecular-targeted drugs have shown clinical activity against SCLC [11]. Identification of genomic aberrations linked to SCLC would facilitate the identification of potential therapeutic targets.

We conducted the present Shizuoka Lung Cancer Mutation Study to assess genomic aberrations in patients with thoracic malignancies. A biobank system was established in collaboration with a clinic pathology lab in July 2011. Mutational data were communicated to clinicians and utilized for assigning patients to appropriate therapy and/or enrolling them in clinical trials. Here we report the genomic aberrations identified in patients with SCLC in the Shizuoka study.

2. Materials and methods

2.1. Patients

We collected samples of SCLC from a biobank system and analyzed these to determine their molecular profiles. To evaluate the relationships between any genomic aberrations and patient characteristics, we collected patient demographic and clinical data from medical records. All patients who participated in this study provided their written informed consent.

Pathological diagnoses were made by institutional pathologists according to the 2004 World Health Organization classification based on morphology (uniform round to spindle-shaped small cells, sparse cytoplasm, high mitotic index, and necrotic areas). The diagnosis of SCLC was confirmed when necessary by immunohistochemical analyses of neuroendocrine markers (synaptophysin, chromogranin A, and CD56). And when it is difficult to diagnose samples as SCLC, we additionally performed immunohistochemistry with makers, such as CAM5.2, TTF-1 and Keratin. If more than 10% of a sample comprised adenocarcinoma, the patient was diagnosed with combined SCLC and adenocarcinoma. Surgically resected samples were macrodissected before nucleic acid extraction and tumor biopsy samples with 10% or more tumor cell component were tested for mutational profiling [12]. All of pleural effusion samples were confirmed that malignant cells were present in each pleural effusion by cytology and we analyzed the cytologically confirmed pleural effusion specimens subsequently.

Smokers were defined according to the Brinkman index (BI) as light (BI value < 600) or heavy (BI value ≥ 600) smokers. Limited stage-disease was defined as disease confined to one hemithorax, the ipsilateral supraclavicular fossa, or both. Disease not meeting these criteria was defined as extended-stage disease. Serum neuron-specific enolase (NSE) levels were measured using a solid-phase radioimmunoassay (RIA) method (SRL Inc., Tokyo, Japan), and progastrin-releasing peptide (Pro-GRP) levels were measured using an enzyme-linked immunosorbent assay (ELISA) kit (FUJIREBIO Inc., Tokyo, Japan).

2.2. Clinical genotyping

We developed a multiplexed tumor genotyping platform to assess 23 mutations in nine genes (*EGFR*, *KRAS*, *BRAF*, *PIK3CA*, *NRAS*, *MEK1*, *AKT1*, *PTEN*, and *HER2*), *EGFR*, *MET*, *PIK3CA*, *FGFR1*, and *FGFR2* amplifications, and *EML4-ALK*, *KIF5B-RET*, *CD74-ROS1*, and *SLC34A2-ROS1* fusion genes (Table 1).

Table 1
Multiplexed tumor genotyping panel.

Gene name	Position	AA mutant	Nucleotide mutant
EGFR	G719	G719	2155G>T/A
		G719A	2156G>C
	exon 19	Deletion	
	T790	T790M	2369C>T
	exon 20	Insertion	
	L858	L858R	2573T>G
	L861	L861Q	2582T>A
KRAS	G12	G12C/S/R	34G>T/A/C
		G12V/A/D	35G>T/C/A
	G13	G13C/S/R	37G>T/A/C
		G13D/A	38G>A/C
	Q61	Q61K	181C>A
		Q61R/L	182A>G/T
		Q61H	183A>T/C
BRAF	G466	G466V	1397G>T
	G469	G469A	1406G>C
	L597	L597V	1789C>G
	V600	V600E	1799T>A
PIK3CA	E542	E542K	1624G>A
	E545	E545K/Q	1633G>A/C
	H1047	H1047R	3140A>G
NRAS	Q61	Q61K	181C>A
		Q61L/R	182A>T/G
MEK1 (MAP2K1)	Q56	Q56P	167A>C
	K57	K57N	171G>T
	D67	D67N	199G>A
AKT1	E17	E17K	49G>A
PTEN	R233	R233*	697C>T
HER2	exon 20	Insertion	

2.3. Nucleic acid sample preparation

DNA samples were extracted from surgically resected tissues, body cavity fluids, and tumor biopsy sections using a QIAamp DNA mini kit (QIAGEN, Hilden, Germany) or a QIAamp DNA formalin-fixed paraffin-embedded (FFPE) tissue kit (QIAGEN). The DNA concentration was measured using a Quant-iT PicoGreen dsDNA assay kit (Invitrogen, Carlsbad, CA). Total RNAs were isolated with an RNeasy Mini kit (QIAGEN) and measured using a spectrophotometer (NanoDrop 2000C; Thermo Scientific, Wilmington, DE).

2.4. Pyrosequencing

Pyrosequencing was used to detect single base substitution-type mutations. An internal fragment of each gene was amplified by polymerase chain reaction (PCR) using primers specific for each gene and a PyroMark PCR kit (QIAGEN). The resulting PCR products were sequenced with the PyroMark Q24 (QIAGEN) pyrosequencer using PyroMark Gold Q96 reagents (QIAGEN) and sequencing primers specific for each gene.

2.5. Fragment analysis

Insertion/deletion-type mutations were identified by sizing the PCR-amplified products using capillary electrophoresis (QIAxcel, QIAGEN).

2.6. Gene copy number analysis

Copy number was evaluated by quantitative real-time PCR (qRT-PCR) performed on a StepOnePlus Real time PCR system (Applied

Biosystems) using SYBR® Premix Ex Taq™ II (Tli RNaseH Plus) (TAKARA BIO) and PCR primers for each gene. If the gene copy number from the samples was more than double that of the cell line known to be normal human genomic DNA, it was considered as evidence of amplification. Detailed methods are described previously [12].

2.7. Screening for transcripts of fusion genes

Fusion genes were detected by multiplex RT-PCR. Synthesis of cDNA templates was performed with total RNA (1 μg) using Oligo $(dT)_{12-18}$ Primer (Invitrogen) and Omniscript RT (QIAGEN) kits. *EML4-ALK* and *ROS1* fusion genes were detected according to the methods of Sun et al. [13] and Li et al. [14], respectively. Methods for the detection of *KIF5B-RET* fusions were kindly provided by Dr. Takashi Kohno (National Cancer Center, Tokyo).

2.8. Statistical analysis

All categorical variables were analyzed by the chi-square test or Fisher's exact test, as appropriate. Continuous variables, including tumor markers, were analyzed using the Mann–Whitney test. All *p*-values were reported to be two-sided, and values of <0.05 were considered statistically significant. All statistical analyses were performed using JMP version 9.0 software (SAS Institute Inc., Cary, NC, USA). Our study was approved by the Institutional Review Board.

3. Results

3.1. Patient characteristics

Between July 2011 and January 2013, SCLC samples from 60 patients were assessed for genomic aberrations. The patient characteristics are shown in Table 2. The median age (range) was 69 (43–82) years, and most patients were male (83%) and heavy smokers (80%). Only two patients were never-smokers. A total of 57 patients were diagnosed with SCLC, while three were diagnosed with combined SCLC and adenocarcinoma. Thirty-one patients had limited-stage disease and 29 had extended-stage disease. We analyzed eight surgically resected snap-frozen samples, 50 FFPE samples, and seven pleural effusion samples. Five patients provided two specimens: three provided both FFPE and surgically resected snap-frozen samples and two provided both FFPE and pleural effusion samples (Table 3).

Table 2
Patients characteristics that were analyzed in our study (overall, *N* = 60).

	N = 60	%
Median age (years)	69	
Range	43–82	
Gender		
Male	50	83
Female	10	17
Smoking status		
Never	2	3
Light (B.I. < 600)	10	17
Heavy (B.I. ≥ 600)	48	80
Histology		
Small cell carcinoma	57	95
Combined small cell carcinoma with adenocarcinoma	3	5
Disease extent		
Limited stage	31	52
Extended stage	29	48
Samples		
Surgically resected snap-frozen samples	8	
FFPE samples	50	
Pleural effusion	7	

Abbreviation: B.I., Brinkman Index; FFPE, Formalin-fixed paraffin-embedded.

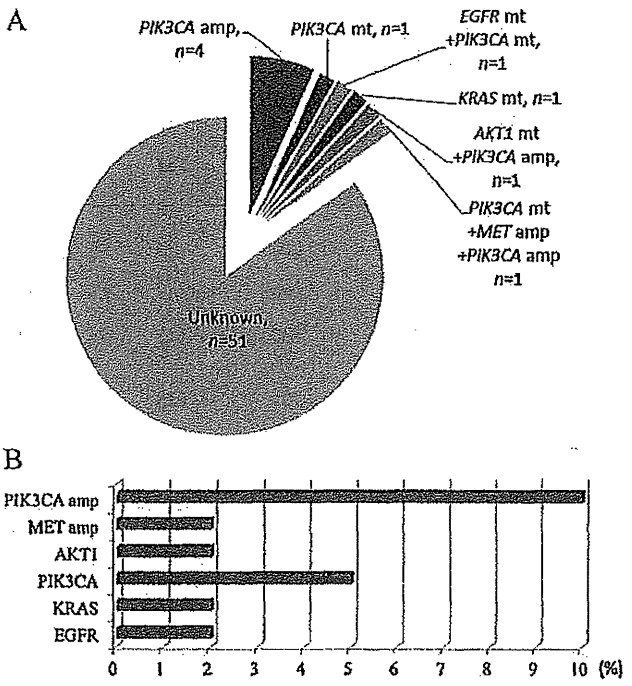

Fig. 1. Relative proportions of genomic aberrations in small cell lung cancer (*N* = 60). (A) Pie chart shows relative proportions of genomic aberrations. (B) Bar chart shows relative proportions of genomic aberrations. *Abbreviations:* mt: mutation; amp: amplification.

3.2. Genomic aberrations

We detected 13 genomic aberrations in nine cases (15%): an *EGFR* mutation (*n* = 1, G719A), a *KRAS* mutation (*n* = 1, G12D), *PIK3CA* mutations (*n* = 3; E542K, E545K, E545Q), an *AKT1* mutation (*n* = 1, E17K), a *MET* amplification (*n* = 1), and *PIK3CA* amplifications (*n* = 6; Fig. 1A and B).

Table 4 shows the individual characteristics of the SCLC patients who harbored genomic aberrations. Eight of the nine patients with genomic aberrations were male, and all were smokers. Two patients were diagnosed with SCLC combined with adenocarcinoma; an *EGFR* mutation was detected in one patient and a *KRAS* mutation in another. The patient with the *EGFR* mutation provided both FFPE and surgically resected snap-frozen samples, but the *EGFR* mutation was detected only in the snap-frozen samples. Genomic aberrations were detected in nine of the 50 FFPE samples, one of eight surgically resected snap-frozen samples, and none of the seven pleural effusion samples.

3.3. Comparison of patient characteristics and genomic aberrations

Patient characteristics are classified by genomic aberration status in Table 4. No significant differences in age, sex, disease extent at diagnosis, or smoking status were found between patients with and without genomic aberrations according to univariate analysis. However, serum NSE and Pro-GRP levels at diagnosis were significantly higher in patients without genomic aberrations than in those with genomic aberrations ($p = 0.02$ and $p = 0.04$, respectively).

Table 3
Patients characteristics that genomic aberrations were detected.

	Age	Gender	B.I.	Disease extent	TNM stage	Samples	Pathology	Genomic aberrations
1	73	Male	2760	LS	IA	FFPE	Small cell carcinoma	PIK3CA amp (3.14)
2	69	Male	1880	LS	IIA	FFPE	Small cell carcinoma	PIK3CA amp (4.42)
3	82	Male	1500	LS	IIIA	FFPE	Small cell carcinoma	PIK3CA amp (2.65)
4	58	Male	1000	ES	IV	FFPE	Small cell carcinoma	PIK3CA (E545K)
5	69	Male	940	LS	IIIA	FFPE	Small cell carcinoma	AKT1 (E17K), PIK3CA amp (2.49)
6	66	Male	840	ES	IIIB	FFPE	Small cell carcinoma	PIK3CA (E542K), MET amp (4.13), PIK3CA amp (3.62)
7	73	Male	795	LS	IIB	FFPE, snap-frozen samples	Small cell carcinoma combined with adenocarcinoma	EGFR (G719A), PIK3CA (E545Q)
8	74	Male	590	ES	IV	FFPE	Small cell carcinoma combined with adenocarcinoma	KRAS (G12D)
9	80	Female	500	LS	IIA	FFPE	Small cell carcinoma	PIK3CA amp (2.78)

Abbreviations: LS, limited stage; ES, extended stage; FFPE, formalin-fixed paraffin-embedded.

Table 4
Patients characteristics classified by genomic aberration status.

	Genomic aberration		*P* value
	Detected	Not detected	
N (%)	9 (15%)	51 (85%)	
Age at diagnosis (years)			0.26
Median	73	69	
Range	58–82	43–82	
Gender, *n* (%)			0.63
Male	8 (89%)	42 (82%)	
Female	1 (11%)	9 (18%)	
Disease extent at diagnosis, *n* (%)			0.32
Limited stage	6 (67%)	25 (49%)	
Extended stage	3 (33%)	26 (51%)	
Smoking status			0.78
Never	0	2	
Light (B.I. < 600)	2	8	
Heavy (B.I. ≥ 600)	7	41	
Serum neuron-specific enolase (NSE) level at diagnosis			0.02
n	9	48	
Median	14	37.1	
Range	7.8–34	6.4–334	
Serum pro-gastrin releasing peptide (Pro-GRP) level at diagnosis			0.04
n	8	47	
Median	75.5	738	
Range	43.1–1500	26.4–65900	

Abbreviation: B.I., Brinkman index.

4. Discussion

As per our knowledge, this was the first molecular profiling report of Asian patients with SCLC, wherein we detected genomic aberrations in 15% patients. *PIK3CA* amplifications were detected in 10% of all samples assessed, while *PIK3CA* mutations were detected in 5%. *PIK3CA genomic aberrations were detected in eight of the* nine patients with genomic aberrations. Recently, two independent comprehensive genomic studies of SCLC were published [15,16]. Peifer et al. [14] analyzed 99 SCLC specimens using 6.0 SNP array analyses and exome, transcriptome, and genome sequencing. They detected *TP53* and *RB1* alterations in 88% and 66% cases, respectively, *MYC* family member and *FGFR1* amplifications in 16% and 6% cases, respectively, and *CREBBP* and *EP300* and *PTEN* mutations in 18% and 10% cases, respectively. They did not detect any *PIK3CA* aberrations. Rudin et al. [15] analyzed 80 SCLC samples, including SCLC cell lines, using multiple exome sequencing, single genome analysis, genome-wide copy-number analysis, and whole-transcriptome sequencing and detected *TP53* and *RB1* mutations in 77% and 31% samples, respectively, a *SOX2* amplification in 27%, and a recurrent *RLF-MYCL1* fusion in 9%. In their study, *PIK3CA* mutation was detected in 2 of 30 primary SCLC tumor samples by exome capture *followed by next generation sequencing (Rudin's report online* methods). Recently, Umemura et al. undertook a comprehensive genomic analysis of SCLC in Japanese patients [17]. They analyzed 51 surgically resected SCLC samples using whole exome sequencing and copy-number analysis. Genetic alterations in the *PI3K* pathway (*PIK3CA, PTEN, AKT2, AKT3, RICTOR, mTOR*) were detected in 17 of 47 samples (36%). *PIK3CA* mutations were detected in three of the 47 samples (6%), which is consistent with the findings from our study.

Okudela et al. reported that *PIK3CA* amplification was detected in 1 of 3 samples (33.3%) and *PIK3CA* gene mutation was detected in

1 of 5 samples (20%) in Japanese patients with SCLC [18]. Although *PIK3CA* mutation is the major genomic aberration in Japanese SCLC patients, the larger study, such as our study and Umemura's report, detected it in approximately 5% of SCLC samples. Based on these results, there does not seem to be significant ethnic differences in the prevalence of *PIK3CA* mutation and *PIK3CA* mutation may be one of the major genomic alterations for the SCLC patients. The *PI3K* pathway plays a central role in cell proliferation and survival in human cancer [19]. The *PIK3CA* gene encodes a class IA PI3K catalytic subunit p110α and is frequently mutated in some of the most common human tumors [20]. Wojtalla et al. showed that approximately 25% primary SCLC tissue samples overexpress the PI3K isoform p110α [21]. They also reported that targeting PI3K p110α affected the proliferation of SCLC cells *in vitro* and *in vivo* and that p110α inhibition led to impaired SCLC tumor formation and vascularization *in vivo*. Many drugs targeting class IA PI3K have been developed [22], and preclinical studies have shown these to have potent antitumor activity. Some have led to a decrease in advanced solid tumors in phase I studies [23,24]; therefore, *PIK3CA* may be a suitable target for the treatment of SCLC.

EGFR and *KRAS* mutations were detected in the patients with combined SCLC and adenocarcinoma in our study. Tatematsu et al. analyzed 122 SCLC patients and detected *EGFR* mutations in 5 (4%) [25]. Their study included 15 combined subtype patients, and 20% of these had *EGFR* mutations. Compared with conventional SCLC, *EGFR* mutations are found significantly more frequently in the combined subtype. Fukui et al. retrospectively studied six patients with combined SCLC and adenocarcinoma and analyzed the *EGFR* mutation status in the microdissected SCLC and adenocarcinoma components of their resected samples [26]. In their report, one of six patients had a missense mutation in *EGFR* (L858R), and both the SCLC and adenocarcinoma components shared the same mutation. Gene mutation status in tissue samples from SCLC with other histology component remain an open question. Therefore it is necessary to perform microdissection in the future study. To the best of our knowledge, there has been no previous report of *KRAS* mutations in SCLC. In our study, a *KRAS* mutation was detected in one patient with combined SCLC and adenocarcinoma.

No significantly different characteristics were found between patients with and without genomic aberrations in the present study. Although the associations between serum tumor markers and genomic aberrations were unclear, serum NSE and pro-GRP levels at diagnosis were significantly lower in the patients with genomic aberrations. Pujol et al. reported that pro-GRP levels did not have any independent prognostic significance [27], while NSE levels have been shown to have better prognostic value [28]. We could not detect an association between prognosis and genomic aberration status (data not shown). Further studies are needed to clarify the relationships between genomic aberrations and serum tumor marker values.

In this study, genomic aberrations were detected in 18% FFPE samples and 13% surgically resected snap-frozen samples. The National Comprehensive Cancer Network (NCCN) guideline recommends that surgery should only be considered for patients with stage I SCLC. However, another report stated that only 5% patients with SCLC have true stage I SCLC [29]. Because surgery is not performed in most patients with SCLC, FFPE samples play a key role in detecting genomic aberrations. Kenmotsu et al. reported on the concordance between FFPE samples and surgically resected snap-frozen samples in multiplexed molecular profiling of lung cancers [30]. Complete concordance of driver mutations was shown for 65% FFPE and snap-frozen samples. These findings indicate that it may be better to analyze FFPE samples to identify SCLC molecular profiles and treat patients with molecular-targeted drugs such as PI3K inhibitors.

Our study had several limitations. First, we analyzed SCLC genomic aberrations using a nine-gene tumor genotyping panel, not a comprehensive panel. In addition, we did not include some known driver mutations such as *TP53* and *RB1* mutations in the panel. However, the objectives of our study were not only to assess the frequency of genomic aberrations but also to detect genomic aberrations that are treatable with targeted drugs, and our multiplexed tumor genotyping platform includes almost all known gene aberrations that are targeted by drugs. And detection of gene amplification may also require consideration of incorporating FISH for future studies. Second, we only analyzed 60 SCLC patients because we only began to analyze genomic aberrations in July 2011. However, other reports have also included a small number of samples. We continue to analyze SCLC samples and utilize the findings for targeted therapy of patients with SCLC.

5. Conclusions

In conclusion, genomic aberrations were found in 15% SCLC patients, with *PIK3CA* amplifications being frequently detected. We previously reported our massive parallel sequencing findings for non-SCLC [31], and we plan to undertake a similar analysis of SCLC samples. A larger study is necessary to further our understanding of the molecular profiles of SCLC.

Conflicts of interest

None of the authors have any financial or personal relationship with other individuals or organizations that could inappropriately influence this study.

Acknowledgments

This study was supported by the Japan Society for the Promotion of Science KAKENHI Grants 24591186 (NY) and 24501363 (YK).

We thank all the patients who participated in this study as well as their families. We also thank Ms. Mie Yamada (Division of Thoracic Oncology, Shizuoka Cancer Center) for data management; Mr. Isamu Hayashi and Mr. Masato Abe (Division of Pathology, Shizuoka Cancer Center) and Ms. Akane Naruoka and Ms. Junko Suzuki (Division of Drug Discovery and Development, Shizuoka Cancer Center Research Institute) for sample preparation and analysis; and Dr. Tomohiro Maniwa, Dr. Masashi Nagata, Dr. Yoshikane Yamauchi, Dr. Naoko Miyata, Dr. Hideaki Kojima, Dr. Yoshiki Kozu, Dr. Chihiro Yamatani, Dr. Kazuo Nakagawa, and Dr. Haruhiko Kondo (Division of Thoracic Surgery) and Dr. Hisao Imai, Dr. Hiroaki Akamatsu, Dr. Takuya Oyakawa, Dr. Yasushi Hisamatsu, Dr. Ryo Ko, Dr. Shota Omori, Dr. Kazuhisa Nakashima, Dr. Takehito Shukuya, Dr. Yukiko Nakamura, Dr. Asuka Tsuya, Dr. Madoka Kimura, Dr. Takaaki Tokito, Dr. Hirofumi Eida, and Dr. Chikara Sakaguchi (Division of Thoracic Oncology, Shizuoka Cancer Center) for their contributions to this study.

References

[1] van Meerbeeck JP, Fennell DA, De Ruysscher DK. Small-cell lung cancer. Lancet 2011;378(9804):1741–55.
[2] Puglisi M, Dolly S, Faria A, Myerson JS, Popat S, O'Brien ME. Treatment options for small cell lung cancer – do we have more choice? Br J Cancer 2010;102(4):629–38.
[3] Lynch TJ, Bell DW, Sordella R, Gurubhagavatula S, Okimoto RA, Brannigan BW, et al. Activating mutations in the epidermal growth factor receptor underlying responsiveness of non-small-cell lung cancer to gefitinib. N Engl J Med 2004;350(21):2129–39.
[4] Paez JG, Janne PA, Lee JC, Tracy S, Greulich H, Gabriel S, et al. EGFR mutations in lung cancer: correlation with clinical response to gefitinib therapy. Science 2004;304(5676):1497–500.
[5] Mitsudomi T, Morita S, Yatabe Y, Negoro S, Okamoto I, Tsurutani J, et al. Gefitinib versus cisplatin plus docetaxel in patients with non-small-cell lung cancer

harbouring mutations of the epidermal growth factor receptor (WJTOG3405): an open label, randomised phase 3 trial. Lancet Oncol 2010;11(2):121–8.
[6] Maemondo M, Inoue A, Kobayashi K, Negoro S, Okamoto I, Tsurutani J, et al. Gefitinib or chemotherapy for non-small-cell lung cancer with mutated EGFR. N Engl J Med 2010;362(25):2380–8.
[7] Zhou C, Wu YL, Chen G, Feng J, Liu XQ, Wang C, et al. Erlotinib versus chemotherapy as first-line treatment for patients with advanced EGFR mutation-positive non-small-cell lung cancer (OPTIMAL CTONG-0802): a multicentre, open-label, randomised, phase 3 study. Lancet Oncol 2011;12(8):735–42.
[8] Rosell R, Carcereny E, Gervais R, Vergnenegre A, Massuti B, Felip E, et al. Erlotinib versus standard chemotherapy as first-line treatment for European patients with advanced EGFR mutation-positive non-small-cell lung cancer (EURTAC): a multicentre, open-label, randomised phase 3 trial. Lancet Oncol 2012;13(3):239–46.
[9] Ettinger DS, Akerley W, Borghaei H, Chang AC, Cheney RT, Chirieac LR, et al. Non-small cell lung cancer. J Natl Compr Cancer Netw 2012;10(10):1236–71.
[10] Peters S, Adjei AA, Gridelli C, Reck M, Kerr K, Felip E. Metastatic non-small-cell lung cancer (NSCLC): ESMO Clinical Practice Guidelines for diagnosis, treatment and follow-up. Ann Oncol 2012;23(Suppl. 7):vii56–64.
[11] Planchard D, Le Pechoux C. Small cell lung cancer: new clinical recommendations and current status of biomarker assessment. Eur J Cancer 2011;47(Suppl. 3):S272–83.
[12] Serizawa M, Koh Y, Kenmotsu H, Isaka M, Murakami H, Akamatsu H, et al. Assessment of mutational profile of Japanese lung adenocarcinoma patients by multitarget assays: a prospective single-institute study cancer; 2014 (in press).
[13] Sun Y, Ren Y, Fang Z, Li C, Fang R, Gao B, et al. Lung adenocarcinoma from East Asian never-smokers is a disease largely defined by targetable oncogenic mutant kinases. J Clin Oncol 2010;28(30):4616–20.
[14] Li C, Fang R, Sun Y, Han X, Li F, Gao B, et al. Spectrum of oncogenic driver mutations in lung adenocarcinomas from East Asian never smokers. PLoS ONE 2011;6(11):e28204.
[15] Peifer M, Fernandez-Cuesta L, Sos ML, George J, Seidel D, Kasper LH, et al. Integrative genome analyses identify key somatic driver mutations of small-cell lung cancer. Nat Genet 2012;44(10):1104–10.
[16] Rudin CM, Durinck S, Stawiski EW, Poirier JT, Modrusan Z, Shames DS, et al. Comprehensive genomic analysis identifies SOX2 as a frequently amplified gene in small-cell lung cancer. Nat Genet 2012;44(10):1111–6.
[17] Umemura S, Goto K, Mimaki S, Ishii G, Ohmatsu H, Niho S, et al. Comprehensive genomic analysis of small cell lung cancer in Asian patients. ASCO Meet Abstr 2013;31(Suppl. 15):7512.
[18] Okudela K, Suzuki M, Kageyama S, Bunai T, Nagura K, Igarashi H, et al. PIK3CA mutation and amplification in human lung cancer. Pathol Int 2007;57(10):664–71.
[19] Luo J, Manning BD, Cantley LC. Targeting the PI3K-Akt pathway in human cancer: rationale and promise. Cancer Cell 2003;4(4):257–62.
[20] Samuels Y, Wang Z, Bardelli A, Silliman N, Ptak J, Szabo S, et al. High frequency of mutations of the PIK3CA gene in human cancers. Science 2004;304(5670):554.
[21] Wojtalla A, Fischer B, Kotelevets N, Mauri FA, Sobek J, Rehrauer H, et al. Targeting the phosphoinositide 3-kinase p110-alpha isoform impairs cell proliferation, survival, and tumor growth in small cell lung cancer. Clin Cancer Res 2013;19(1):96–105.
[22] Liu P, Cheng H, Roberts TM, Zhao JJ. Targeting the phosphoinositide 3-kinase pathway in cancer. Nat Rev Drug Discov 2009;8(8):627–44.
[23] Gonzalez-Angulo AM, Juric D, Argiles G, Schellens JH, Burris HA, Berlin J, et al. Safety, pharmacokinetics, and preliminary activity of the α-specific PI3K inhibitor BYL719: results from the first-in-human study. ASCO Meet Abstr 2013;31(Suppl. 15):2531.
[24] Omlin AG, Spicer JF, Sarker D, Pinato DJ, Agarwal R, Cassier PA, et al. A pharmacokinetic (PK) pharmacodynamic (PD) driven first-in-human study of the oral class I PI3K inhibitor CH5132799, in patients with advanced solid tumors. ASCO Meet Abstr 2012;30(Suppl. 15):3022.
[25] Tatematsu A, Shimizu J, Murakami Y, Horio Y, Nakamura S, Hida T, et al. Epidermal growth factor receptor mutations in small cell lung cancer. Clin Cancer Res 2008;14(19):6092–6.
[26] Fukui T, Tsuta K, Furuta K, Watanabe S, Asamura H, Ohe Y, et al. Epidermal growth factor receptor mutation status and clinicopathological features of combined small cell carcinoma with adenocarcinoma of the lung. Cancer Sci 2007;98(11):1714–9.
[27] Pujol JL, Quantin X, Jacot W, Boher JM, Grenier J, Lamy PJ. Neuroendocrine and cytokeratin serum markers as prognostic determinants of small cell lung cancer. Lung Cancer 2003;39(2):131–8.
[28] Jorgensen LG, Osterlind K, Genolla J, Gomm SA, Hernandez JR, Johnson PW, et al. Serum neuron-specific enolase (S-NSE) and the prognosis in small-cell lung cancer (SCLC): a combined multivariable analysis on data from nine centres. Br J Cancer 1996;74(3):463–7.
[29] Ignatius Ou SH, Zell JA. The applicability of the proposed IASLC staging revisions to small cell lung cancer (SCLC) with comparison to the current UICC 6th TNM Edition. J Thorac Oncol 2009;4(3):300–10.
[30] Kenmotsu H, Serizawa M, Koh Y, Isaka M, Takahashi T, Murakami H, et al. Concordance between formalin-fixed paraffin-embedded biopsy samples and surgically resected snap-frozen samples in multiplexed molecular profiling of lung cancers. ASCO Meet Abstr 2013;31(Suppl. 15):e18556.
[31] Koh Y, Kenmotsu H, Serizawa M, Isaka M, Mori K, Imai H, et al. Identification of actionable mutations in surgically resected tumor specimens from Japanese patients with non-small cell lung cancer by ultra-deep targeted sequencing. ASCO Meet Abstr 2013;31(Suppl. 15):7572.

Watanabe et al. Journal of Translational Medicine 2014, 12:143
http://www.translational-medicine.com/content/12/1/143

JOURNAL OF TRANSLATIONAL MEDICINE

METHODOLOGY Open Access

A novel flow cytometry-based cell capture platform for the detection, capture and molecular characterization of rare tumor cells in blood

Masaru Watanabe[1,2], Masakuni Serizawa[1], Takeshi Sawada[3], Kazuo Takeda[4], Toshiaki Takahashi[5], Nobuyuki Yamamoto[2,5], Fumiaki Koizumi[3] and Yasuhiro Koh[1,2*]

Abstract

Background: Personalized cancer treatment relies on the accurate detection of actionable genomic aberrations in tumor cells. Circulating tumor cells (CTCs) could provide an alternative genetic resource for diagnosis; however, the technical difficulties in isolating and analyzing rare CTCs have limited progress to date. In this preclinical study, we aimed to develop an improved capture system for molecular characterization of CTCs based on a novel cell sorting technology.

Methods: We developed a cell capture platform using On-chip Sort (On-Chip Biotechnologies), a novel bench-top cell sorter equipped with a disposable microfluidic chip. Spike-in experiments comprising a series of lung cancer cell lines with varying epithelial cell adhesion molecule (EpCAM) expression levels were conducted to assess the capture and purification efficiency of the platform. Samples were negatively enriched using anti-CD45-coated magnetic beads to remove white blood cells, followed by sample fixation and labeling. The enriched and labeled samples were then sorted by On-chip Sort based on cytokeratin, vimentin, and CD45 expression. Captured cells were immediately subjected to whole genome amplification followed by mutation analysis using deep targeted sequencing, and copy number analysis using quantitative polymerase chain reaction (qPCR).

Results: Spike-in experiments revealed an excellent overall mean capture rate of 70.9%. A 100% success rate in the detection of *EGFR*, *KRAS* and *BRAF* mutations from captured cells was achieved using pyrosequencing and deep sequencing. The mutant variant detection rates were markedly higher than those obtained with the CellSearch profile kit. qPCR analysis of amplified DNA demonstrated reproducible detection of copy number changes of the *EGFR* in captured tumor cells.

Conclusions: Using a novel cell sorter, we established an efficient and convenient platform for the capture of CTCs. Results of a proof-of-principle preclinical study indicated that this platform has potential for the molecular characterization of captured CTCs from patients.

Keywords: Circulating tumor cells, Cell sorter, Flow cytometry, Liquid biopsy, EpCAM-independent, Next-generation sequencing, Mutation detection, Single cell analysis, Whole genome amplification

* Correspondence: ykoh@wakayama-med.ac.jp
[1]Drug Discovery and Development Division, Shizuoka Cancer Center Research Institute, Shizuoka, Japan
[2]Third Department of Internal Medicine, Wakayama Medical University, Wakayama, Japan
Full list of author information is available at the end of the article

Background

Recent advances in molecularly targeted cancer therapy have offered up a wide variety of therapeutic strategies. The presence or absence of various actionable genomic aberrations has been shown to predict response to molecularly targeted treatments [1]. In some cases, identification of genetic aberrations is a prerequisite for commencing treatment; for example, identification of *EGFR*-activating mutations in patients with non-small cell lung cancer is required prior to starting treatments with EGFR tyrosine kinase inhibitors [2]. However, kinase inhibition frequently leads to the appearance of drug resistance mutations within the target kinase itself, such as the EGFR T790M mutation [3].

In addition to identifying gene mutations, there is also a need for detection of protein expression and gene amplification of targeted molecules on primary tumor cells for further stratification of patients [4]. To optimize treatment, real-time monitoring of tumors over the course of the treatment, especially at the point of treatment failure, is necessary. However, rebiopsy remains challenging, mainly because of the invasiveness of the procedure.

Circulating tumor cells (CTCs) could potentially serve as an alternative to tumor tissue as a source of material for the detection of genetic alterations, an approach that is termed "liquid biopsy" [5-11] owing to its minimal invasiveness. To date, the CellSearch system (Veridex LLC, Raritan, NJ, USA) is the only United States Food and Drug Administration-approved CTC enumeration system for the provision of prognostic information regarding survival [12-17]. However, the isolation of the rare CTCs for molecular analysis remains technically challenging. Most of the currently available capture methods retain a considerable number of white blood cells (WBCs) and cell loss during sample handling. Various methods to overcome this issue have been under development and evaluation [18-28].

The conventional cell sorting device is a well-established cell capture system and it has previously been used to enrich CTCs from whole blood [29]. However, it is reportedly difficult to efficiently carry out this isolation when using blood samples with a low CTC count together with a conventional fluorescence-activated cell sorter [20].

Recently, we have established a protocol for CTCs enumeration using a newly-developed flow cytometry FISHMAN-R [30]. The results of preclinical study showed superior sensitivity of their system in detecting EpCAM-negative tumor cells in direct comparison with the standard method. This protocol also enables a detection of EpCAM−/CK− cells and epithelial-mesenchymal transition (EMT)-induced tumor cells using the incorporation of an EMT marker [30]. The system and protocol have been evaluated and validated for the enumeration of CTCs in clinical feasibility study [31,32].

In this study, we introduced a new approach for the characterization of CTCs captured by On-chip Sort cell sorter. This novel cell sorter is an integrated sorting unit with FISHMAN-R, allowing the detection and isolation of rare tumor cells for subsequent molecular analyses. Here we evaluate the feasibility of mutation analysis of the isolated rare cell in blood after immunomagnetic enrichment and fluorescence-activated cell sorting. This is an efficient and convenient platform based on a cell sorting system, and promising preclinical results were obtained for possible future clinical application.

Methods

Cell lines and culture

The tumor cell lines A431, A549, H292, HCC827, H1975, and H1755 were obtained from the American Type Culture Collection (ATCC; Lockville, MD). The breast cancer cell line Hs578T was kindly gifted by Dr. Tohru Mochizuki (Shizuoka Cancer Center Research Institute, Japan). A549, H292, HCC827, H1975, and H1755 cells were cultured in RPMI-1640 (Invitrogen, Carlsbad, CA) containing 10% fetal bovine serum (Gibco, Life Technologies, Grand Island, NY). A431 and Hs578T cells was cultured in Dulbecco's modified Eagle's medium (DMEM; Invitrogen) containing 10% FBS. Cell lines were cultured under humidified 5% CO_2/95% air at 37°C.

Blood spiking experiments

Blood samples of 4 mL each were spiked with 5–25 cells of the above-mentioned cell lines and were used for the isolation of tumor cells for mutation and gene copy number analysis. Blood samples were collected from healthy volunteers working at Shizuoka Cancer Center who consented to donation. This study was approved by the independent institutional review board of Shizuoka Cancer Center.

Tumor cells were harvested by incubation with 0.25% trypsin/EDTA (Gibco) solution for several minutes at 37°C, and then washed and resuspended in T-buffer {0.5% bovine serum albumin (Nacalai Tesque Inc., Kyoto, Japan) and 2 mM ethylenediaminetetraacetic acid (EDTA; Sigma-Aldrich, St. Louis, MO), and 0.5% Through Path Plus (On-Chip Biotechnologies, Tokyo, Japan) in phosphate-buffered saline (PBS, Invitrogen)} to obtain a final concentration of 10^2 cells/100 μL. From this suspension, tumor cells were individually picked up using a micropipette under an inverted microscope, and subsequently added to the 4 mL healthy blood sample. These spiked samples were then processed immediately via immunomagnetic enrichment as described below.

Immunomagnetic enrichment and sample staining procedures

Immunomagnetic enrichment and sample staining of cells were described previously [30]. Briefly, samples

were negatively enriched using Dynabeads coated with anti-CD45 monoclonal antibody (Invitrogen) to remove white blood cells, followed by fixation and labeling with the fluorescein isothiocyanate (FITC)-conjugated anti-CK mAb CK3-6H5 (1:25 dilution; Miltenyi Biotec, Bergisch-Gladbach, Germany), the PE-conjugated anti-vimentin mAb D21H3 (1:50 dilution; Cell Signaling Technology, Danvers, MA), and the Alexa Fluor 700-conjugated anti-CD45 mAb F10-89-4 (1:20 dilution; AbD Serotec, Oxford, UK). Samples were incubated overnight at 4°C in the dark, followed by stained with 1 μg/mL Hoechst 33342 (Sigma-Aldrich, St. Louis, MO) for 10 min at RT in the dark.

On-chip Sort cell sorter

The novel cell sorter used in this study, On-chip Sort (On-Chip Biotechnologies, Tokyo, Japan), is a bench-top size sorter that is compatible with operation in most biosafety cabinets (Figure 1A). As shown in Figure 1B, the disposable microfluidic chip contains all fluidic and optical paths within a single, closed system, which is intended to realize cross contamination-free, biosafety adherent, lossless whole volume sorting. This system therefore provides suitable conditions for the capture of CTCs in a clinical setting. The principle of sorting will be described elsewhere.

The On-chip Sort of this paper has two excitation lasers (blue; 473 nm, 10 mW and red; 640 nm, 30 mW) and four detection channels, FL2 (509–552 nm), FL3 (565–605 nm), FL4 (576-620 nm), FL5 (658–695 nm), and FL6 (>700 nm). Signals for FITC, PE, Alexa Fluor 647, and Alexa Fluor 700 were collected through these detection channels. Voltages of each light sensor module of each channel are optimized for CTC detection (FSC: gain Low, SSC: 0.25 V, FL2: 0.35 V, FL3: 0.33 V, FL4:0.35 V, FL5: 0.48 V, and FL6: 0.35 V). On-chip Sort software version 24.1 (On-Chip Biotechnologies) was used for signal acquisition. Data analysis was performed using FlowJo software v7.6.5 (Tree Star, Inc, Ashland, OR).

Enumeration and sorting procedures

Enumeration and sorting of cells were performed by On-chip Sort according to the manufacturer's instructions. Briefly, the flow path was pre-washed with the 1 × Through Path Plus (On-Chip Biotechnologies) and the On-chip sample buffer (1 × Through Path Plus with 1.5% polyvinylpyrrolidone, On-Chip Biotechnologies). Stained samples were dissolved in 25 μL to 100 μL of On-chip sample buffer and then a flow rate was up to 150 events/sec (about 1 μL/min: 1.8 kPa in the On-chip Sort setting). Total events were approximately 1×10^5 to 10^6 events. The sorting time required for all the samples was approximately 30 to 120 minutes depending on the final sample volume.

The sorted cells gated into the cytokeratin and/or vimentin positive and CD45 negative channels were collected into

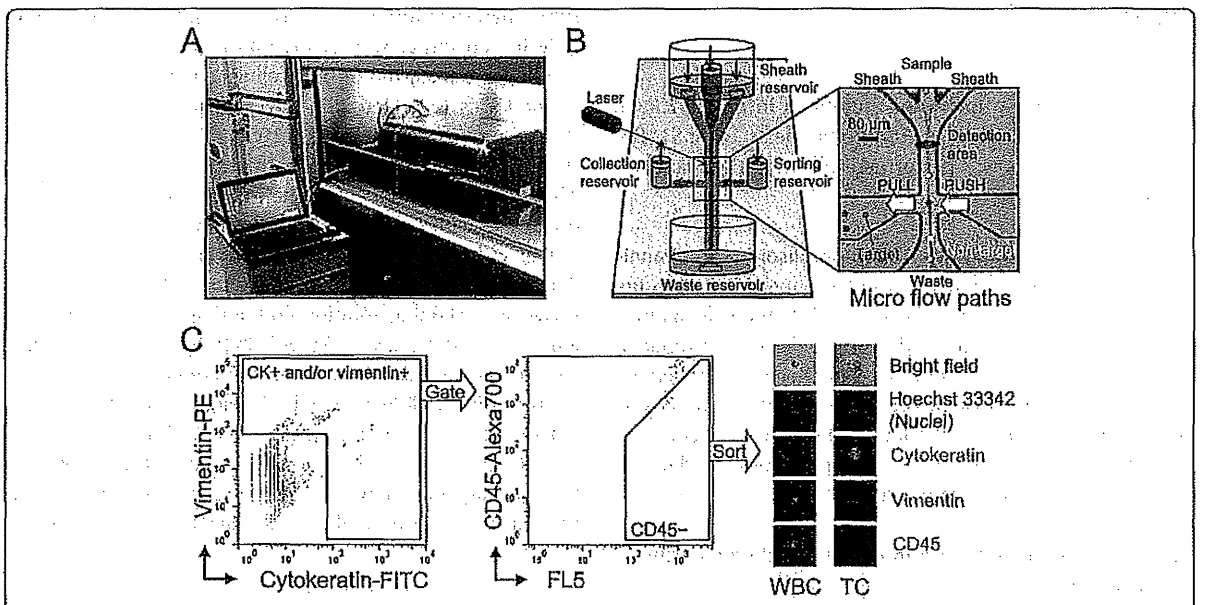

Figure 1 Cell sorter instrument and gating mechanism for tumor cells. (A) Image of the On-chip Sort cell sorter. (B) Image of the disposable microfluidic chip used. The chip is self-contained with both inlet and outlet sample/sheath reservoirs, which ensures that no fluids come into contact with the device. The target cells are separated to the collection reservoir by this shift of flow alone. A magnified view of the micro flow paths is shown in the inset on the right. (C) Sorting gates for spiked tumor cells. Tumor cells gated as cytokeratin + and/or vimentin+/CD45− were sorted. Nuclei, cytokeratin, vimentin and CD45 staining was used to distinguish tumor cells (Tumor cell, TC; nuclei+/CK+ and/or vimentin+/CD45−) from the white blood cell population (White blood cell, WBC; nuclei+/CK−/vimentin+/CD45+).

the collection reservoir, and then observed under a fluorescence microscope (Biorevo BZ-9000: Keyence, Osaka, Japan) to confirm that the cells were nucleated (nuclear stain-positive), cytokeratin and/or vimentin positive and CD45 negative. All steps were carried out at room temperature.

Whole genome amplification

Sorted cells were transferred from the collection reservoir to a 200 μL polymerase chain reaction (PCR) tube and rinsed the collection reservoir with sheath solution twice. After centrification (600 x g for 10 min), the supernatant was carefully aspirated to leave ~1 μL, which comprised the starting volume of the whole genome amplification (WGA) procedure. WGA was performed using the *Ampli*1 WGA kit (Silicon Biosystems, Bologna, Italy) following the manufacturer's protocol. The AMPure XP PCR Purification Kit (Beckman Coulter, Beverly, MA) was used to clean up the amplified DNA, and DNA concentrations were determined using a NanoDrop spectrophotometer (NanoDrop Technologies, Waltham, MA, USA). Quality control checks of the WGA product were performed using the *Ampli*1 QC Kit (Silicon Biosystems). Only samples positive for four PCR products were considered to contain successfully amplified genomic material suitable for mutation analysis. Amplified DNA product of 2, 20 or 250 ng was subjected to mutation analysis using quantitative real-time-PCR (qPCR) amplification, pyrosequencing, or deep sequencing, respectively.

Pyrosequencing

The amplification primers for mutations in *EGFR*, *KRAS*, and *BRAF* are described in Additional file 1: Table S1. Pyrosequencing PCR was performed following the manufacturer's instructions.

Deep sequencing using the TruSeq Amplicon Cancer Panel

A total of 48 genes frequently mutated in cancer according to the COSMIC database (Catalogue Of Somatic Mutations In Cancer), were sequenced using a TruSeq Amplicon Cancer Panel (TSACP; Illumina, San Diego, CA) following the manufacturer's instructions. Variant call analysis was performed with Amplicon Viewer (Illumina). Coverage information was obtained using CLC genomics Workbench 6.0 (CLC Bio, Aarhus, Denmark).

Mutation analysis of lung tumor cells enriched with the CellSearch profile kit.

To compare the cell capture performance of the On-chip Sort platform versus the CellSearch platform (Veridex LLC), nine tubes (three regular 5 mL blood collection tubes containing EDTA) of blood were collected from a healthy volunteer. H1975, A549 or H1755 tumor cells were spiked into the 5 mL of blood to a final concentration of 10 cells/mL. Two blood collection tubes (total of 10 mL blood) were delivered to an independent medical laboratory (Genetic Lab, Sapporo, Japan). There, tumor cell capture was performed using the CellSearch profile kit (Veridex LLC) or the On-chip Sort in parallel concurrently. Captured samples using the CellSearch profile kit were stored in a CellSave Preservative Tube (Veridex LLC) and sent back to our laboratory. After a single wash with T-buffer, samples were stained as described above. Captured samples using the On-chip Sort were stored at 4°C until the initiation of WGA in parallel with returned CellSearch samples. Both samples were subjected to WGA concurrently, followed by mutation analysis.

Gene copy number analysis for *EGFR*

qPCR amplification of the *EGFR* was performed on the StepOnePlus Real-time PCR system (Applied Biosystems, Foster City, CA) using SYBR Premix Ex Taq II (Tli RNase H Plus; Takara Bio, Shiga, Japan). The amplification primers used are described in Additional file 1: Table S1.

Immunoblot analysis and immunofluorescence staining

Immunoblot analysis was as described previously [33]. Briefly, the cultured tumor cells were harvested and lysed in lysis buffer (50 mM Tris-HCl, pH 7.4, 50 mM NaCl, 1% Nonidet P-40, 2 mM EDTA, 10 mM NaF, 2 mM sodium orthovanadate and protease inhibitor cocktail). Whole cell lysate was electrophoresed on a 12% SDS-PAGE gel, transferred to nitrocellulose membrane (Bio-Rad Laboratories Inc., Hercules, CA) and immunoblotted with the a the phospho-EGFR (Tyr1068, D7A5; Cell Signaling), the EGFR (D38B1; Cell Signaling), or α-tubulin (YL1/2; Millipore, Temecula, CA). The intensity of the bands was quantified with ImageJ (Wayne Rasband, NIH, MD).

The cultured tumor cells were harvested and fixed. After washing with T-buffer once, the cell pellet was dissolved in a staining solution containing the PE-conjugated anti-CD326 (EpCAM) mAb 9C4 (1:25 dilution, BioLegend, San Diego, CA) or Alexa Fluor 647-conjugated anti-EGFR mAb D38B1 (Cell Signaling Technology). Samples were incubated overnight at 4°C in the dark. Unbound antibodies were removed via washing with 2 mL of T-buffer followed by centrifugation. Flow cytometry was performed using the On-chip Sort. Data analysis was performed using FlowJo software v7.6.5.

Statistical analysis

Prism software (GraphPad Software, Inc., La Jolla, CA) was used for statistical analyses. Statistical significance of difference was determined using the unpaired Student's *t*-test.

Results

Assay development for CTC detection and capture after negative depletion enrichment

To capture CTCs in whole blood, we used a novel cell sorter, On-chip Sort (Figure 1). Discrimination of CTCs from the bulk of the blood cells was achieved by negative enrichment using anti-human CD45 microbeads [30]. A typical example for the full gating strategy is shown in Figure 1C. Gating of the CTCs by On-chip Sort was carried out using the CK-FITC staining vs. the vimentin-PE staining density plot (Figure 1C, left). The lower limit of the gate that discriminates CTC signals from WBCs autofluorescence as well as from debris was determined by several runs of non-spike experiments using healthy donor control bloods (Additional file 2: Figure S1). The CK+ and/or vimentin+ events were then subjected to CD45 negative gating to distinguish tumor cells from WBCs and/or debris. Tumor cell events that appeared in the CD45-Alexa Fluor 700 vs. FL5 density plot (FL5 is a detection channel adjacent to that for Alexa Fluor 700) were easily distinguished from the WBCs and debris population (Figure 1C, middle).

Immunofluorescence staining of the On-chip Sort sorted cells identified these cells as nuclei, CK and/or vimentin-positive and CD45-negative under the fluorescent microscope, confirming these cells to be tumor cells. Tumor cells were easily distinguished from WBC, which were CD45-positive and CK-negative (Figure 1C, right). Five healthy donor control samples were processed with above settings (Additional file 2: Figure S1). On average these samples have 1.2 ± 1.3 events in the CTC gate. However no sorted tumor cells (CK+ and/or vimentin+, CD45− cells) were observed.

Evaluation of captured tumor cells from spiked blood samples

To assess the performance of our method, low numbers (i.e., 5, 13, or 25 cells) of various non-small cell lung tumor H1975, A549 or H1755 cells expressing varying levels of EpCAM were spiked into 4 mL of normal blood, and processed according to our protocol for tumor cell isolation with the On-chip Sort system. As shown in Figure 2A, H1975 cells displayed high EpCAM expression, whereas A549 cells exhibited partial EpCAM expression. H1755 cells did not appear to express any EpCAM.

Results of the sorting experiments are summarized in Figure 2B and in Additional file 3: Table S2. Overall, the mean percentages of cells detected into the gate as shown in Figure 1C were 86.9% ± 8.6%, 84.7% ± 9.3%, and 83.4% ± 12.4% for H1975, A549, and H1755 cells, respectively ($n = 9$). These detection rates are comparable to those obtained in the previous report using FISHMAN-R [30]. Captured cells into collecting reservoir were confirmed to be tumor cells using microscopy of cell morphology and positive CK and vimentin fluorescent labeling, while contaminating cells were identified by cell morphology and positive CD45 staining (Additional file 4: Figure S2). Overall mean percentages of cells captured were 68.5% ± 9.2%, 69.8% ± 9.9%, and 74.5% ± 12.7% for H1975, A549, and H1755 cells, respectively. Observation of CD45-positive cells under the fluorescent microscope yielded a purity of captured tumor cells after cell isolation with On-chip Sort of 78.4% ± 13.9%, 69.8% ± 18.5% and 70.4% ± 12.4% for H1975, A549, and H1755 cells, respectively.

Regression analysis of the number of detected tumor cells versus the number of expected tumor cells produced a correlation coefficient (R^2) of 0.9978, 0.9967 and 0.9965 for H1975, A549, and H1755 cells, respectively (Figure 2C, blue line). The number of captured tumor cells was also highly linear, with a correlation coefficient of $R^2 = 0.9928$, 0.9985 or 0.9963 in H1975, A549, or H1755 cells, respectively (Figure 2C, red line).

Validation of mutation detection methods

Prior to performing mutation analysis on tumor cells captured with On-chip Sort, we tested whether WGA products are usable for sequencing by pyrosequencing and deep sequencing methods. The H1975 human lung tumor cell line harboring known mutations in the *EGFR* was used. Two single cells and two groups of ten cells each were analyzed for the presence of two different mutations in the *EGFR*; using both pyrosequencing and deep sequencing subsequent to the WGA procedure. Both mutations were reliably detected by pyrosequencing even in single cells, as well as in both unamplified and amplified H1975 genomic DNA carried out as a positive control (Table 1). These *EGFR* mutations were not detected in any of the amplified WBC samples carried out as a negative control (Table 1).

Amplicon libraries were generated using the TSACP followed by deep sequencing with an Illumina MiSeq sequencer. Significant single nucleotide variants (occurring in > 1% of DNA in the sample) were found in both the small groups of cells as well as in the single cells with satisfactory sequence coverage depth (Table 1). Similarly, A549 and H1755 human lung tumor cell lines harboring known mutations in the *KRAS* and *BRAF* were also reliably called with sufficient variant frequency when using small numbers of cells as well as in single cells (Additional file 5: Table S3).

Analytical sensitivities of pyrosequencing and deep sequencing were analyzed by titration studies using normal leukocyte and *EGFR* mutant H1975 cells. One or ten mutant cells were mixed with wild-type cells (normal leukocytes) in dilutions of 20, 5, and 1% of mutant cells. All cell mixtures were subjected to WGA, followed by sequencing with pyrosequencing and deep sequencing.

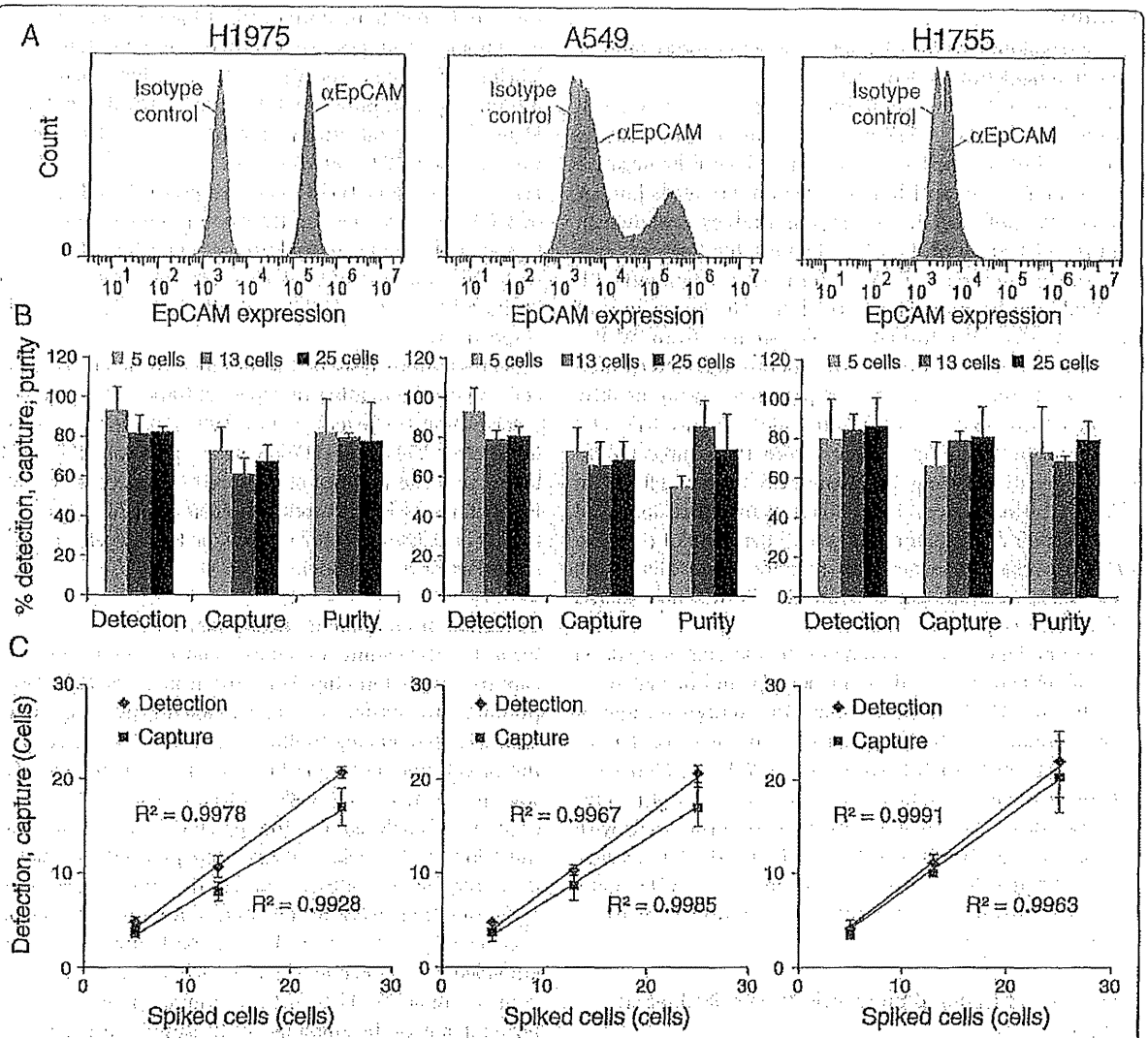

Figure 2 Performance of On-chip Sort in a spike-in experiment. (A) Histograms of EpCAM expression in H1975, A549, and H1755 non-small cell lung tumor cell lines. Fluorescence histograms of the isotype control (gray) and of the EpCAM antibody (red). (B) The mean percent detection, capture and purity of 5, 13, and 25 tumor cells isolated following spiking into 4 mL of normal blood ($n = 3$). The number of detected tumor cells was calculated using FlowJo software. The number of captured tumor cells was counted as the number of cells found in the collection reservoir. Purity was calculated as the number of captured tumor cells divided by the number of captured tumor cells plus white blood cells counted in the collection reservoir. (C) Linearity of tumor cell detection (blue lines) and capture (red lines) in spiking experiments. Error bars represent S.D. of the mean. Data shown here are representative of two independent experiments for each assay.

Results are shown in Additional file 6: Figure S3. Even at mutant cell dilutions of 1%, the deep sequencing method was capable of detecting mutations in *EGFR* (Additional file 6: Figure S3B), while pyrosequencing had a lower detection limit of 10% (Additional file 6: Figure S3A).

Mutation analysis of captured tumor cells

To enable the mutation analysis of CTCs isolated with On-chip Sort, the sorted lung tumor cell samples shown in Figure 2 were analyzed for the presence of specific mutations in each cell line using pyrosequencing and deep sequencing. Variant frequencies were compared with those of both unamplified and amplified H1975 genomic DNA samples. Results of the mutation analysis of the cells sorted for WGA and the purity of these samples are summarized in Additional file 3: Table S2. All expected mutations were reliably detected in all sorted samples with sufficient coverage, with none detected in the amplified WBC samples. These results suggest that even where tumor cells were present at concentrations as low as five cells per 4 mL of blood, they could be successfully isolated using On-chip Sort, amplified genome DNA by

Table 1 Mutation analysis of single or small groups of tumor cells

Cells	Template	EGFR mutation	Var. Freq. by Pyro.	Var. Freq. by MiSeq		Coverage min. = 10× (212 amplicons)
				Var. Freq.	Total read	
H1975	Unamplified gDNA	L858R (2573T>G)	75%	78.2%	13,070	100.0%
		T790M (2369C>T)	74%	79.5%	11,044	
H1975	Amplified gDNA	L858R	73%	65.9%	372	96.7%
		T790M	72%	75.2%	10,013	
H1975	10 cells	L858R	71%	88.8%	4,479	92.0%
		T790M	79%	84.1%	27,539	
H1975	10 cells	L858R	73%	90.1%	601	93.5%
		T790M	77%	80.9%	35,070	
H1975	1 cell	L858R	68%	77.1%	109	90.6%
		T790M	79%	87.0%	31,312	
H1975	1 cell	L858R	69%	78.2%	368	80.2%
		T790M	61%	63.8%	27,341	
WBC from healthy donor	10 cells	L858R	2%	N/A	3,596	81.4%
		T790M	0%	N/A	18,497	
WBC from healthy donor	1 cell	L858R	3%	N/A	56	88.7%
		T790M	0%	N/A	256	

Footnote: Tumor cells or normal WBCs were fixed and stained followed by *Ampli*1 WGA. WGA products were sequenced using a pyrosequencer or the Illumina MiSeq sequencer. Variant frequencies of two different mutations in the *EGFR* and the coverage distribution of WGA products using the TSACP are shown. Pyro., psyrosequence Var. Freq., variant frequency. Coverage min., coverage minimum.

WGA, and profiled by deep sequencing with sufficient depth.

We further evaluated whether On-chip Sort was capable of capturing very low number of tumor cells in blood. 4 mL blood samples containing one or two H1975 cells were processed with On-chip Sort in 6 independent tests (Additional file 7: Table S4). The results demonstrated a sensitivity threshold for On-chip Sort platform detecting close to one tumor cell per 4 mL of blood. In addition, tumor cells were not detected from healthy donor blood containing no tumor cells. Therefore, CTCs could be detected and isolated form patients who have ≥1 CTCs per 4 mL of blood by the On-chip Sort platform and they could be genotyped utilizing isolated CTCs.

We also found that EpCAM/CK double-negative Hs578T cells spiked into healthy blood were successfully isolated with On-chip Sort and profiled by mutation analysis (Additional file 8: Figure S4); the resulting mutation profiles showed the expected genomic mutation in p53 known to be present in Hs578T. These results strongly suggest that our CTC capture assay is advantageous for capturing and characterizing both EpCAM-positive and EpCAM-negative tumor cells.

Comparative analysis of On-chip sort versus the CellSearch profile kit

We next performed a comparative analysis of On-chip Sort versus the CellSearch profile kit in terms of mutation detection of tumor cells spiked into blood samples. Cells isolated using On-chip Sort or the CellSearch profile kit were processed by WGA followed by mutation analysis with pyrosequencing or deep sequencing. In On-chip Sort-isolated samples, specific mutations in each tumor cell line were reliably detected by both pyrosequencing and deep sequencing (Figure 3, left). In CellSearch profile kit-isolated samples however, specific mutations in H1975 cells expressing high EpCAM levels were detected by deep sequencing only and not by pyrosequencing (Figure 3, right). In both experiments, genomic DNA was successfully amplified according to *Ampli*1 end-point PCR criteria in all of the samples (Additional file 9: Figure S5). Details of the mutation analysis are shown in Additional file 10: Table S5. These data suggest that the On-chip Sort assay provides superior sensitivity compared with the CellSearch profile kit for subsequent mutation detection.

Assessment of EGFR expression and copy number amplification in captured tumor cells

Owing to the multichannel detection capability of the system, EGFR expression levels on single CTCs are measurable and semi-quantifiable using an anti-EGFR antibody in the FL5 channel of On-chip Sort. We first performed experiments to demonstrate that EGFR immunostaining on On-chip Sort could be correlated to EGFR expression and gene amplification status as determined by western

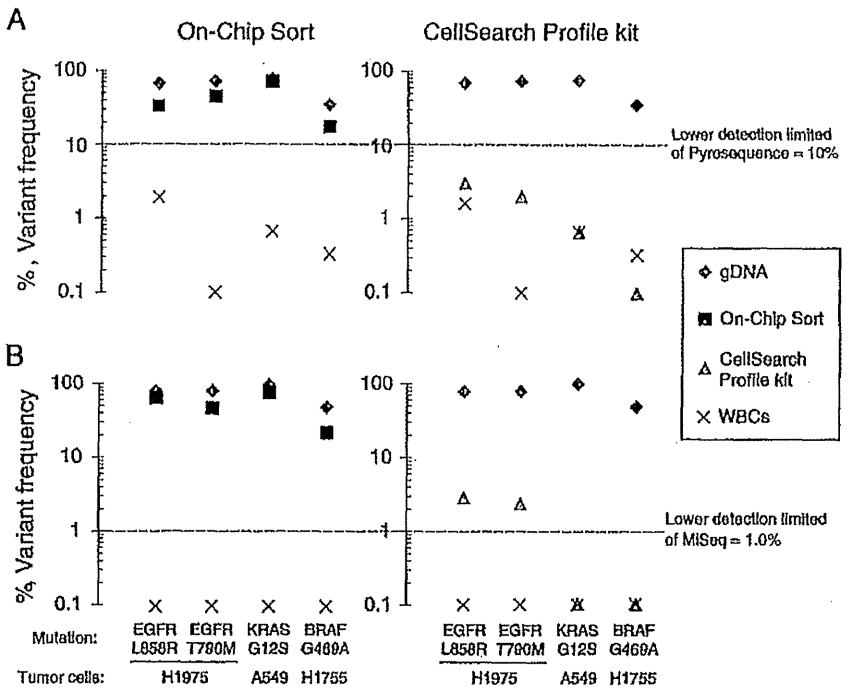

Figure 3 Head-to-head comparison of On-chip Sort with the CellSearch profile kit. Three tumor cell lines (H1975, A549 and H1755) expressing varying levels of EpCAM were spiked into blood from a healthy donor (10 cells/mL). The samples were divided into three and then processed using our On-chip Sort protocol as well as the CellSearch profile kit in parallel. Captured tumor cells were subjected to whole genome amplification followed by mutation detection with both pyrosequencing and deep sequencing to detect specific mutations in each tumor cell. Variant frequencies detected in the controls (gDNA and WBCs from a healthy donor) and experimental samples using pyrosequencing **(A)** or deep sequencing **(B)** are graphically represented. The line represents the lower limit of detection of each method (10% for pyrosequencing and 1% for deep sequencing). Samples with 0% variant frequency were assigned a value of 0.1 for plotting purposes. Data shown here are representative of two independent experiments for each assay.

blot analysis and qPCR using WGA products from various cell lines. To distinguish different levels of EGFR protein expression and *EGFR* amplification, we used the EGFR-over-expressing and/or EGFR-amplified cell lines H292, A431, and HCC827 (Figure 4A, C). Very low-level EGFR-expressing A549 cells with a single *EGFR* copy served as a negative control (Figure 4A, C).

A549 cells were either weakly positive or negative, whereas H292 cells also revealed moderate EGFR expression (Figure 4B). In A431 and HCC827 cells, strong intensities of EGFR specific immunofluorescence were observed (Figure 4B). These EGFR expression levels correlated with those determined by immunoblot analysis (Figure 4A). CTCs with moderate to strong intensities of EGFR-specific immunofluorescence were assumed to be EGFR-positive (H292, A431, and HC827), whereas CTCs with negative or only weak intensities of EGFR-specific immunofluorescence were considered to be EGFR-negative (A549) (Figure 4B).

EGFR expression levels determined using On-chip Sort were consistent with the mean gene amplifications determined by qPCR carried out on DNA extracts of the corresponding cell lines (Figure 4C, black bars; A549, 1.18-fold; H292, 1.69-fold; A431, 6.32-fold; HCC827, 25.37-fold). In line with these results, the analysis of *Ampli*1 WGA products of genomic DNA (1 ng) and of small numbers of cells including single cells, by *EGFR* qPCR, revealed comparable mean values in the respective cell lines (Figure 4C, grey bars). The mean gene amplifications of pure tumor cell samples (Figure 4C, grey bars) and of those isolated by On-chip Sort (Figure 4C, blue bars) were compared, and found to be reasonably similar to that observed in the cell lines with strong expression levels of EGFR (A431 and HC827; Figure 4C), whereas no significant amplification was detected in H292, which expresses moderate levels of EGFR (Figure 4C). The results of these sorting experiments are summarized in Additional file 11: Table S6.

Discussion

In this study, we have described a new approach for the capture of rare tumor cells from immunomagnetically pre-enriched blood samples. We provided proof-of-principle demonstrating the feasibility of this approach by using it to capture between one and ten tumor cells from spiked blood samples for subsequent

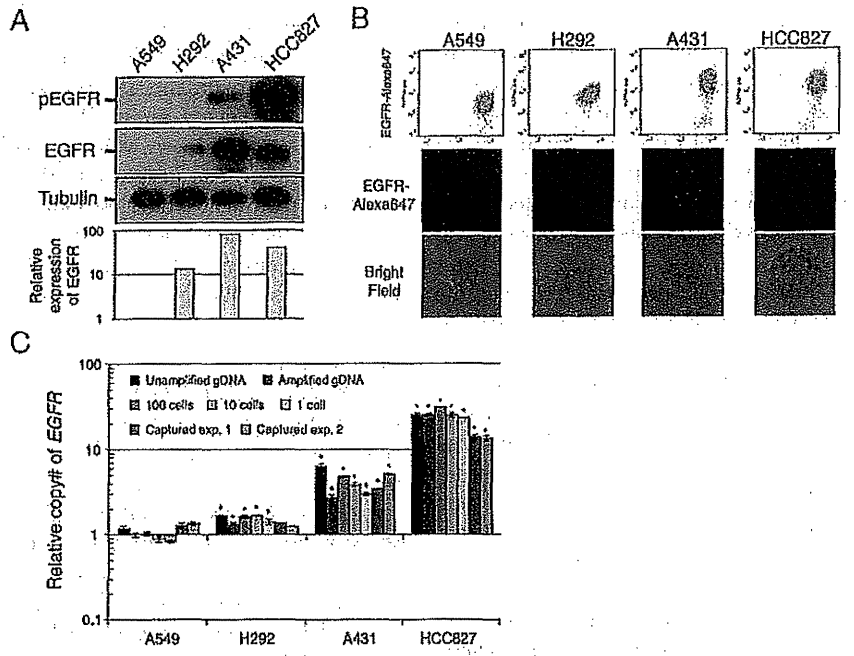

Figure 4 EGFR protein expression and *EGFR* amplification in tumor cells captured by On-chip Sort. (A, B) EGFR protein expression detected by western blot (A), correlated with EGFR protein expression captured by On-chip Sort (B), for A549 low EGFR expression and no EGFR amplification, H292 (moderate EGFR expression and amplification rate), A431 (strong EGFR expression and amplification rate), and HCC827 (strong EGFR expression and large amplification rate) cell lines. (C) Comparison of *EGFR* amplification rates determined by qPCR with gDNA (black bar), and when using *Ampli*1 WGA products (gray bars) including WGA of captured tumor cells (blue bars).

molecular characterization at the genomic level using deep sequencing.

In addition, we investigated the applicability of using WGA products obtained from single CTCs with the *Ampli*1 WGA kit. This WGA kit is the only commercially available kit compatible with analysis of a single fixed cell. Fixation is a crucial step for the staining of cytokeratin and vimentin with fluorescent probes, and cytokeratin positivity is included to gold standard criteria for CTC detection. The WGA/sequencing procedure described in this study was shown to be serviceable for the detection of a broad range of somatic mutations in 48 cancer-related genes in small numbers of cells, as well as in single cells for the first time. A coverage depth of 10-fold was achieved even for single cells at >90% of the nucleotide positions. Next-generation sequencing-based diagnostics may therefore hold the potential to provide clinically relevant information using single CTCs.

Total CTC capture yield is important in genotyping as well as in other applications, such as prognostic and drug response measurements. The overall mean percentage of cells captured was 70.9% ± 10.6% ($n = 27$). The percentage of cell loss attributed to the negative enrichment procedure and sorting was about 20% and 10%, respectively. The estimated capture limit of the number of tumor cells captured by our system was 1.46 ± 0.22 CTCs/4 mL blood. The cut-off number of CTC events detected by the On-chip Sort method was 3 events/4 mL blood (Additional file 2: Figure S1), suggesting that the CTC capture efficiency of our system to detect mutation might be sufficient for low CTC cohort numbers. In fact, we were able to detect specific mutations from blood samples containing one tumor cell.

In a low CTC cohort (<15 CTCs/7.5 mL), the rate of successful subsequent WGA was reported to be 23.5% ($n = 34$) after isolation using a conventional cell sorter [20]. Cell loss during sample handling is a critical issue in CTC isolation when using CellSearch [21,28]. Unlike conventional cell sorters and CellSearch, the On-chip Sort system employs a lossless whole volume sorting approach, and as a result, displays 100% successful subsequent WGA as well as mutation detection of spiked blood samples as low as five tumor cells in 4 mL blood ($n = 9$).

Purity of isolated CTCs is also crucial for obtaining high sensitivity in mutation detection. The On-chip Sort system isolated tumor cells at a purity of >60%, which is sufficient for mutation detection using pyrosequencing methods that have a sensitivity of approximately 10%. When directly comparing mutation detection sensitivity of our system with that of the CellSearch system and profile kit, our system was observed to be significantly more sensitive at low CTC numbers (<10 CTCs/mL).

Detection of variant frequency of *EGFR* mutations in high EpCAM-expressing H1975 cells after our sorting procedure was approximately 68%, which was sufficient to call the mutations. However, in the same samples using the CellSearch system, variant frequency was approximately 3%, which is insufficient for unambiguous variant identification. These results suggest that our system displays superior purification efficiency for the detection of mutations using the relatively low-sensitivity downstream pyrosequencing method.

The use of EMT markers, e.g., vimentin, facilitated the capture of EpCAM/CK double-negative tumor cell in peripheral blood. The loss of EpCAM and/or CK in tumor cells has been reported previously [34-39]. This loss of epithelial cell properties is related to Epithelial-to-Mesenchymal Transition (EMT). Our multicolor cell sorting system allows us to capture a CTC-positive marker and an EMT-related marker in parallel, suggesting that a population of CTCs that has been missed by current platforms might be able to capture and characterize using our system. However, vimentin is also expressed on mesenchymal stromal cells which normally circulate [40]. Criteria for vimentin+ CTCs must be carefully defined and evaluated in future clinical studies. We also consider using other EMT-related makers such as N-cadherin or twist in addition to vimentin staining to detect and capture CTCs which show mesenchymal phenotype [34,38]. Our multicolor cell sorting system equipped with multilaser has the potential to capture CTCs multiple EMT markers. In addition to CTC markers, nuclear staining positivity is regarded one of the golden standard criteria to detect CTCs. It is important to incorporate nuclear positivity in sorting gates to classify the events as CTCs or not in the case of clinical samples. On-chip Sort can be equipped with violet laser for detection of DAPI staining. Further improvement of equipment is needed to be a robust diagnostic tool for cancer patients.

While the use of *Ampli*1 technology has previously been reported for PCR-based mutation analysis on single cells [21,22], qPCR to determine copy number of single cells using the *Ampli*1 kit has not yet been evaluated. In our study, the mean gene amplification rates within various tumor cells determined by qPCR on DNA extracts were similar to those determined with *Ampli*1 WGA products when using both DNA extracts as well as small numbers of cells, including single cells. The amplification of the *EGFR* could also be observed in captured samples, suggesting our system might be capable for detecting gene amplification on CTCs. Such analyses may assist in predictive biomarker studies in cases where expression levels of therapeutic targets may be predictive of therapeutic activity. For example, High EGFR expression of tumor cells was shown to predict the benefit of anti-EGFR therapy such as cetuximab [41].

Evaluation of the clinical feasibility of phenotypic analysis in captured CTCs by evaluating target gene expression is still ongoing. The DETECT III trial assesses the use of anti-HER2 treatments in HER2-negative breast cancer patients selected on the basis of CTC detection/characterization [42], www.detect-studien.de. Results of this trial will give an insight into the relevance of CTCs in cancer treatment strategies. Our system has clear advantages over conventional systems when carrying out longitudinal analyses of CTC dynamics in terms of protein expression as well as of mutation status.

Conclusions

We have provided the first report on the performance of the On-chip Sort system, a novel bench-top cell sorter that allows the capture of low numbers of cells from human blood samples. We have described the analytical characteristics of the system and provided proof-of-principle showing its feasibility in the capture and molecular characterization of low numbers of tumor cells in blood. Ongoing improvement of CTC enrichment processes from whole blood and integration of single-cell technologies may help to establish CTCs as a pivotal diagnostic tool for cancer patients towards enabling better-personalized therapies. The data shown in this study imply the potential of the On-chip Sort cell capture system and further evaluation with clinical samples should be conducted.

Additional files

Additional file 1: Table S1. Primers used for pyrosequencing and quantitative PCR (qPCR). *1: 5′ ends of the amplification primers were biotinylated.

Additional file 2: Figure S1. Detection and sorting data of healthy donor control samples. A typical example of healthy control samples analyzed with On-chip Sort. On average five healthy donor control samples have 1.2 ± 1.3 events ($n = 5$) in the CTC gate (CK+ and/or vimentin+/CD45−), but no tumor cells were observe in the collecting reservoir.

Additional file 3: Table S2. Details of mutation analysis of captured cells. This table provides details of DNA from captured tumor cells shown in Figure 2, which was amplified using *Ampli*1 WGA followed by mutation detection with both a pyrosequencer and an Illumina MiSeq sequencer. Variant frequencies of two different *EGFR* mutations and single *KRAS* and *BRAF* mutations, as well as coverage distribution of WGA products in the TruSeq Amplicon Cancer Panel are shown. Var. Freq., variant frequency. Coverage min., coverage minimum.

Additional file 4: Figure S2. Gallery of H1975 cells captured by On-chip Sort in the collection reservoir. Captured cells are shown with binding to fluorescently-labeled antibodies targeting cytokeratin, vimentin, and CD45. The images allowed for identification of tumor cells (arrow) and hematologic cells (arrowheads).

Additional file 5: Table S3. Mutation analysis of single or small groups of A549 and H1755 cells. Tumor cells were fixed and stained followed by *Ampli*1 WGA. WGA products were sequenced using a pyrosequencer or an Illumina MiSeq sequencer. Variant frequency of *KRAS* or *BRAF* mutations and WGA coverage distribution in the TruSeq Amplicon Cancer Panel are shown. Var. Freq., variant frequency. Coverage min., coverage minimum.

Additional file 6: Figure S3. Analytical sensitivity of mutation detection. Dilutions of *EGFR* mutant H1975 cells spiked into healthy donor WBCs were analyzed by both pyrosequencing and deep sequencing for detection of T790M and L858R mutations. Variant frequencies of *EGFR* mutations detected by the pyrosequencer (A) or MiSeq sequencer (B) are graphically represented. The horizontal axis shows the expected fraction of mutant *EGFR* cells. The vertical axis shows the observed percentage of variant frequency. The variant frequencies of the T790M mutation (diamonds) and of the L858R mutation (squares) are indicated. Blue marks indicate dilutions of single H1975 cell into WBC samples and green marks indicate dilutions of ten H1975 cells into WBC samples. The line represents the lower limit of detection of the method (10% for pyrosequencing and 1% for deep sequencing). Data shown here are representative of two independent experiments for each assay.

Additional file 7: Table S4. Evaluation of sensitivity of On-chip Sort platform for mutation detection. One or two cultured H1975 cells were individually picked up using a micropipette under an inverted microscope, spiked into 4 mL aliquots of healthy donor blood, and the resulting blood samples were processed using the On-chip Sort platform in 6 separate tests. Captured samples were analyzed for the presence of specific mutations in each cell line using pyrosequencing.

Additional file 8: Figure S4. Capture and mutation profiling of CK–/EpCAM – breast cancer cells. (A) Histograms of CK, EpCAM, and vimentin expression in Hs578T cells. Fluorescence histograms of the isotype control (gray) and of the EpCAM antibody (red). (B) CTC gates of spiked Hs578T cells and gallery of Hs578T cells captured by On-chip Sort. The images allowed for identification of Hs578T cells (arrow). (C) Details of sorting results and mutation analysis using deep sequencing. DNA from captured Hs578T cells was amplified using *Ampli*1 WGA followed by mutation detection with an Illumina MiSeq sequencer. Variant frequencies of *p53* mutation and coverage distribution of WGA products in the TSACP are shown. Var. Freq., variant frequency. Coverage min., coverage minimum.

Additional file 9: Figure S5. Composite gel images of *Ampli*1 QC end-point PCR products. Genomic DNA of experimental samples was considered to be successfully amplified if all four of the control genomic DNA sequences were detected. No amplification product was obtained in either of the negative control samples (NTC and Buffer). All of the captured samples obtained using either On-chip Sort or the CellSearch Profile kit passed the *Ampli*1 amplification check. NTC, no template control; gDNA, 1 ng of H1975 gDNA as a positive control for *Ampli*1 QC; Buffer, negative control for WGA.

Additional file 10: Table S5. Details of mutation analysis of captured tumor cells using On-chip Sort or the CellSearch profile kit. This table provides details of the captured sample in Figure 3 that were subjected to mutation analysis. DNA from captured tumor cells were amplified using *Ampli*1 WGA followed by mutation detection using both the pyrosequencer and the Illumina MiSeq sequencer. Variant frequencies of two different *EGFR* mutations, single *KRAS* and *BRAF* mutations, and coverage distribution of WGA products in the TruSeq Amplicon Cancer Panel are shown. Var. Freq., variant frequency. Coverage min., coverage minimum.

Additional file 11: Table S6. Capture efficiencies and purity of tumor cells spiked into 4 mL of normal blood. This table provides details of the captured samples show in Figure 4 that were subjected to copy number analysis. The number of captured tumor cells was counted as the number of tumor cells found in the collection reservoir. Purity was calculated as the number of captured tumor cells divided by the number of captured tumor cells plus the number of white blood cells counted in the collection reservoir ($n = 2$).

Abbreviations

CTCs: Circulating tumor cells; EpCAM: Epithelial cell adhesion molecule; qPCR: Quantitative polymerase chain reaction; WBCs: White blood cells; FITC: Fluorescein isothiocyanate; CK: Cytokeratin; PE: Phycoerythrin; WGA: Whole genome amplification; TSACP: TruSeq Amplicon Cancer Panel.

Competing interests

KT represents the manufacturer of On-chip Sort.

Authors' contributions

MW and YK conceived and designed the experiments. MW performed the experiments except the deep sequencing. MS performed the deep sequencing. MW analyzed the data and conducted the statistical analysis. MS analyzed the coverage data of deep sequencing. MW, MS, TS, KT, TT, NY, FK, and YK contributed reagents, materials, and analysis tools. MW and YK wrote the paper. All authors read and approved the final manuscript.

Acknowledgements

The authors thank Mrs. Junko Suzuki (Shizuoka Cancer Center Research Institute) and Dr. Yukiko Ito and Ms. Misaki Ono (National Cancer Center Hospital) for technical assistance and Dr. Yuu Fujimura, Dr. Namiko Yamashita, and Dr. Masayuki Ishige (On-Chip Biotechnologies) for technical support and helpful comments.
This research was supported by the Advanced Research and Development Project on Diagnosis and Treatment for Early Stage of Cancer, Development of Automatic Testing System for Genetic Diagnosis using Peripheral Blood from New Energy and Industrial Technology Development Organization (NEDO), Japan.

Author details

[1]Drug Discovery and Development Division, Shizuoka Cancer Center Research Institute, Shizuoka, Japan. [2]Third Department of Internal Medicine, Wakayama Medical University, Wakayama, Japan. [3]Shien-Lab, National Cancer Center Hospital, Tokyo, Japan. [4]On-Chip Biotechnologies Co., Ltd., Tokyo, Japan. [5]Division of Thoracic Oncology, Shizuoka Cancer Center Hospital, Shizuoka, Japan.

Received: 4 January 2014 Accepted: 12 May 2014
Published: 23 May 2014

References

1. La Thangue NB, Kerr DJ: Predictive biomarkers: a paradigm shift towards personalized cancer medicine. *Nat Rev Clin Oncol* 2011, 8:587–596.
2. Maemondo M, Inoue A, Kobayashi K, Sugawara S, Oizumi S, Isobe H, Gemma A, Harada M, Yoshizawa H, Kinoshita I, Fujita Y, Okinaga S, Hirano H, Yoshimori K, Harada T, Ogura T, Ando M, Miyazawa H, Tanaka T, Saijo Y, Hagiwara K, Morita S, Nukiwa T, North-East Japan Study Group: Gefitinib or chemotherapy for non-small-cell lung cancer with mutated EGFR. *N Engl J Med* 2010, 362:2380–2388.
3. Kobayashi S, Boggon TJ, Dayaram T, Jänne PA, Kocher O, Meyerson M, Johnson BE, Eck MJ, Tenen DG, Halmos B: EGFR mutation and resistance of non-small-cell lung cancer to gefitinib. *N Engl J Med* 2005, 352:786–792.
4. Moroni M, Veronese S, Benvenuti S, Marrapese G, Sartore-Bianchi A, Di Nicolantonio F, Gambacorta M, Siena S, Bardelli A: Gene copy number for epidermal growth factor receptor (EGFR) and clinical response to anti EGFR treatment in colorectal cancer: a cohort study. *Lancet Oncol* 2005, 6:279–286.
5. Pantel K, Alix-Panabieres C: Circulating tumour cells in cancer patients: challenges and perspectives. *Trends Mol Med* 2010, 16:398–406.
6. Lianidou ES: Circulating tumor cells: new challenges ahead. *Clin Chem* 2012, 58:1–3.
7. Pantel K, Alix-Panabieres C, Riethdorf S: Cancer micrometastases. *Nat Rev Clin Oncol* 2009, 6:339–351.
8. Miller MC, Doyle GV, Terstappen LW: Significance of circulating tumor cells detected by the Cell Search System in patients with metastatic breast colorectal and prostate cancer. *J Oncol* 2010, 2010:617421.
9. Pierga JY, Bidard FC, Mathiot C, Brain E, Delaloge S, Giachetti S, de Cremoux P, Salmon R, Vincent-Salomon A, Marty M: Circulating tumor cell detection predicts early metastatic relapse after neoadjuvant chemotherapy in large operable and locally advanced breast cancer in a phase II randomized trial. *Clin Cancer Res* 2008, 14:7004–7010.
10. Gorges TM, Pantel K: Circulating tumor cells as therapy-related biomarkers in cancer patients. *Cancer Immunol Immunother* 2013, 62:931–939.
11. Heitzer E, Auer M, Ulz P, Geigl JB, Speicher MR: Circulating tumor cells and DNA as liquid biopsies. *Genome Med* 2013, 5:73.
12. Cristofanilli M, Budd GT, Ellis MJ, Stopeck A, Matera J, Miller MC, Reuben JM, Doyle GV, Allard WJ, Terstappen LW, Hayes DF: Circulating tumor cells, disease progression, and survival in metastatic breast cancer. *N Engl J Med* 2004, 351:781–791.

13. Cohen SJ, Punt CJ, Iannotti N, Saidman BH, Sabbath KD, Gabrail NY, Picus J, Morse M, Mitchell E, Miller MC, Doyle GV, Tissing H, Terstappen LW, Meropol NJ: Relationship of circulating tumor cells to tumor response, progression-free survival, and overall survival in patients with metastatic colorectal cancer. *J Clin Oncol* 2008, 26:3213–3221.
14. de Bono JS, Scher HI, Montgomery RB, Parker C, Miller MC, Tissing H, Doyle GV, Terstappen LW, Pienta KJ, Raghavan D: Circulating tumor cells predict survival benefit from treatment in metastatic castration-resistant prostate cancer. *Clin Cancer Res* 2008, 14:6302–6309.
15. Krebs MG, Sloane R, Priest L, Lancashire L, Hou JM, Greystoke A, Ward TH, Ferraldeschi R, Hughes A, Clack G, Ranson M, Dive C, Blackhall FH: Evaluation and prognostic significance of circulating tumor cells in patients with non-small-cell lung cancer. *J Clin Oncol* 2011, 29:1556–1563.
16. Naito T, Tanaka F, Ono A, Yoneda K, Takahashi T, Murakami H, Nakamura Y, Tsuya A, Kenmotsu H, Shukuya T, Kaira K, Koh Y, Endo M, Hasegawa S, Yamamoto N: Prognostic impact of circulating tumor cells in patients with small cell lung cancer. *J Thorac Oncol* 2012, 7:512–519.
17. Matsusaka S, Chin K, Ogura M, Suenaga M, Shinozaki E, Mishima Y, Terui Y, Mizunuma N, Hatake K: Circulating tumor cells as a surrogate marker for determining response to chemotherapy in patients with advanced gastric cancer. *Cancer Sci* 2010, 101:1067–1071.
18. Cann GM, Gulzar ZG, Cooper S, Li R, Luo S, Tat M, Stuart S, Schroth G, Srinivas S, Ronaghi M, Brooks JD, Talasaz AH: mRNA-Seq of single prostate cancer circulating tumor cells reveals recapitulation of gene expression and pathways found in prostate cancer. *PLoS One* 2012, 7:e49144.
19. Powell AA, Talasaz AH, Zhang H, Coram MA, Reddy A, Deng G, Telli ML, Advani RH, Carlson RW, Mollick JA, Sheth S, Kurian AW, Ford JM, Stockdale FE, Quake SR, Pease RF, Mindrinos MN, Bhanot G, Dairkee SH, Davis RW, Jeffrey SS: Single cell profiling of circulating tumor cells: transcriptional heterogeneity and diversity from breast cancer cell lines. *PLoS One* 2012, 7:e33788.
20. Magbanua MJ, Sosa EV, Roy R, Eisenbud LE, Scott JH, Olshen A, Pinkel D, Rugo HS, Park JW: Genomic profiling of isolated circulating tumor cells from metastatic breast cancer patients. *Cancer Res* 2013, 73:30–40.
21. Peeters DJ, De Laere B, Van den Eynden GG, Van Laere SJ, Rothé F, Ignatiadis M, Sieuwerts AM, Lambrechts D, Rutten A, van Dam PA, Pauwels P, Peeters M, Vermeulen PB, Dirix LY: Semiautomated isolation and molecular characterisation of single or highly purified tumour cells from CellSearch enriched blood samples using dielectrophoretic cell sorting. *Br J Cancer* 2013, 108:1358–1367.
22. Fabbri F, Carloni S, Zoli W, Ulivi P, Gallerani G, Fici P, Chiadini E, Passardi A, Frassineti GL, Ragazzini A, Amadori D: Detection and recovery of circulating colon cancer cells using a dielectrophoresis-based device: KRAS mutation status in pure CTCs. *Cancer Lett* 2013, 335:225–231.
23. Gasch C, Bauernhofer T, Pichler M, Langer-Freitag S, Reeh M, Seifert AM, Mauermann O, Izbicki JR, Pantel K, Riethdorf S: Heterogeneity of epidermal growth factor receptor status and mutations of KRAS/PIK3CA in circulating tumor cells of patients with colorectal cancer. *Clin Chem* 2013, 59:252–260.
24. Heitzer E, Auer M, Gasch C, Pichler M, Ulz P, Hoffmann EM, Lax S, Waldispuehl-Geigl J, Mauermann O, Lackner C, Höfler G, Eisner F, Sill H, Samonigg H, Pantel K, Riethdorf S, Bauernhofer T, Geigl JB, Speicher MR: Complex tumor genomes inferred from single circulating tumor cells by array-CGH and next-generation sequencing. *Cancer Res* 2013, 73:2965–2975.
25. Ozkumur E, Shah AM, Ciciliano JC, Emmink BL, Miyamoto DT, Brachtel E, Yu M, Chen PI, Morgan B, Trautwein J, Kimura A, Sengupta S, Stott SL, Karabacak NM, Barber TA, Walsh JR, Smith K, Spuhler PS, Sullivan JP, Lee RJ, Ting DT, Luo X, Shaw AT, Bardia A, Sequist LV, Louis DN, Maheswaran S, Kapur R, Haber DA, Toner M: Inertial focusing for tumor antigen-dependent and -independent sorting of rare circulating tumor cells. *Sci Trans Med* 2013, 5:179ra47.
26. Harb W, Fan A, Tran T, Danila DC, Keys D, Schwartz M, Ionescu-Zanetti C: Mutational Analysis of Circulating Tumor Cells Using a Novel Microfluidic Collection Device and qPCR Assay. *Transl Oncol* 2013, 6:528–538.
27. Earhart CM, Hughes CE, Gaster RS, Ooi CC, Wilson RJ, Zhou LY, Humke EW, Xu L, Wong DJ, Willingham SB, Schwartz EJ, Weissman IL, Jeffrey SS, Neal JW, Rohatgi R, Wakelee HA, Wang SX: Isolation and mutational analysis of circulating tumor cells from lung cancer patients with magnetic sifters and biochips. *Lab Chip* 2013, 14:78–88.
28. Swennenhuis JF, Reumers J, Thys K, Aerssens J, Terstappen LW: Efficiency of whole genome amplification of Single Circulating Tumor Cells enriched by Cell Search and sorted by FACS. *Genome Med* 2013, 5:106.
29. Moreno JG, O'Hara SM, Gross S, Doyle G, Fritsche H, Gomella LG, Terstappen LW: Changes in circulating carcinoma cells in patients with metastatic prostate cancer correlate with disease status. *Urology* 2001, 58:386–392.
30. Watanabe M, Uehara Y, Yamashita N, Fujimura Y, Nishio K, Sawada T, Takeda K, Koizumi F, Koh Y: Multicolor Detection of Rare Tumor Cells in Blood Using a Novel Flow Cytometry-based System. *Cytometry Part A* 2014, 85:206–213.
31. Sawada T, Ito Y, Watanabe M, Fujimura Y, Nakamichi S, Kanda S, Horinouchi H, Fujiwara Y, Nokihara H, Yamamoto N, Tamura T, Koh Y, Koizumi F: Clinical feasibility study of a novel cytometry-based-system for the detection of circulating tumor cells of patients with lung cancer [abstract]. *Cancer Res* 2013, 73:1445.
32. Ito Y, Sawada T, Watanabe M, Fujimura Y, Hashimoto J, Kodaira M, Yunokawa M, Yamamoto H, Yonemori K, Shimizu C, Tamura K, Fujiwara Y, Koh Y, Koizumi F: Detection of circulating tumor cells for malignant epithelial tumor using a novel cytometry-based system [abstract]. *Cancer Res* 2013, 73:1446.
33. Serizawa M, Takahashi T, Yamamoto N, Koh Y: Combined treatment with erlotinib and a transforming growth factor-β type I receptor inhibitor effectively suppresses the enhanced motility of erlotinib-resistant non-small-cell lung cancer cells. *J Thorac Oncol* 2013, 8:259–269.
34. Armstrong AJ, Marengo MS, Oltean S, Kemeny G, Bitting RL, Turnbull JD, Herold CI, Marcom PK, George DJ, Garcia-Blanco MA: Circulating tumor cells from patients with advanced prostate and breast cancer display both epithelial and mesenchymal markers. *Mol Cancer Res* 2011, 9:997–1007.
35. Lecharpentier A, Vielh P, Perez-Moreno P, Planchard D, Soria JC, Farace F: Detection of circulating tumour cells with a hybrid (epithelial/mesenchymal) phenotype in patients with metastatic non-small cell lung cancer. *Br J Cancer* 2011, 105:1338–1341.
36. Pecot CV, Bischoff FZ, Mayer JA, Wong KL, Pham T, Bottsford-Miller J, Stone RL, Lin YG, Jaladurgam P, Roh JW, Goodman BW, Merritt WM, Pircher TJ, Mikolajczyk SD, Nick AM, Celestino J, Eng C, Ellis LM, Deavers MT, Sood AK: A novel platform for detection of CK+ and CK- CTCs. *Cancer Discov* 2011, 1:580–586.
37. Aktas B, Tewes M, Fehm T, Hauch S, Kimmig R, Kasimir-Bauer S: Stem cell and epithelial-mesenchymal transition markers are frequently overexpressed in circulating tumor cells of metastatic breast cancer patients. *Breast Cancer Res* 2009, 11:R46.
38. Kallergi G, Papadaki MA, Politaki E, Mavroudis D, Georgoulias V, Agelaki S: Epithelial to mesenchymal transition markers expressed in circulating tumour cells of early and metastatic breast cancer patients. *Breast Cancer Res* 2011, 13:R59.
39. Yu M, Bardia A, Wittner BS, Stott SL, Smas ME, Ting DT, Isakoff SJ, Ciciliano JC, Wells MN, Shah AM, Concannon KF, Donaldson MC, Sequist LV, Brachtel E, Sgroi D, Baselga J, Ramaswamy S, Toner M, Haber DA, Maheswaran S: Circulating breast tumor cells exhibit dynamic changes in epithelial and mesenchymal composition. *Science* 2013, 339:580–584.
40. Panepucci RA, Siufi JL, Silva WA Jr, Proto-Siquiera R, Neder L, Orellana M, Rocha V, Covas DT, Zago MA: Comparison of gene expression of umbilical cord vein and bone marrow-derived mesenchymal stem cells. *Stem Cells* 2004, 22:1263–1278.
41. Pirker R, Pereira JR, von Pawel J, Krzakowski M, Ramlau R, Park K, de Marinis F, Eberhardt WE, Paz-Ares L, Störkel S, Schumacher KM, von Heydebreck A, Celik I, O'Byrne KJ: EGFR expression as a predictor of survival for first-line chemotherapy plus cetuximab in patients with advanced non-small-cell lung cancer: analysis of data from the phase 3 FLEX study. *Lancet Oncol* 2012, 13:33–42.
42. Bidard FC, Fehm T, Ignatiadis M, Smerage JB, Alix-Panabières C, Janni W, Messina C, Paoletti C, Müller V, Hayes DF, Piccart M, Pierga JY: Clinical application of circulating tumor cells in breast cancer: overview of the current interventional trials. *Cancer Metastasis Rev* 2013, 32:179–188.

doi:10.1186/1479-5876-12-143
Cite this article as: Watanabe *et al.*: A novel flow cytometry-based cell capture platform for the detection, capture and molecular characterization of rare tumor cells in blood. *Journal of Translational Medicine* 2014 12:143.

Efficacy of Rechallenge Chemotherapy in Patients With Sensitive Relapsed Small Cell Lung Cancer

Kazushige Wakuda, MD, Hirotsugu Kenmotsu, MD,* Tateaki Naito, MD, PhD,* Hiroaki Akamatsu, MD,* Akira Ono, MD,* Takehito Shukuya, MD,* Yukiko Nakamura, MD,* Asuka Tsuya, MD PhD,* Haruyasu Murakami, MD, PhD,* Toshiaki Takahashi, MD, PhD,* Masahiro Endo, MD, PhD,† Takashi Nakajima, MD, PhD,‡ and Nobuyuki Yamamoto, MD, PhD**

Objectives: To evaluate the efficacy of rechallenge with current induction regimens for sensitive-relapse small cell lung cancer (SCLC) patients.

Methods: We defined sensitive relapse as treatment-free interval (TFI ≥ 90 d). Sensitive-relapse SCLC patients who received second-line chemotherapy were separated into those treated with rechallenge chemotherapy (rechallenge group) and those treated with other regimens (other group). The endpoints were overall survival (OS), progression-free survival, and toxicity.

Results: Sixty-five patients (19 rechallenge group and 46 other group) were assessable for efficacy and safety evaluation. No significant differences in age, sex, ECOG performance status at relapse, disease extent at diagnosis, or response to first-line treatment were found between the 2 groups, but TFI was significantly longer in the rechallenge group. Twenty-one patients of the other group received amrubicin. There was no significant difference in OS between the 2 groups [median survival time (MST): rechallenge group, 14.4 mo; other group, 13.1 mo; $P=0.51$]. In the patients treated with amrubicin, MST was 12.6 months. Comparing the rechallenge group with the patients treated with amrubicin, there was also no significant difference in OS ($P=0.38$). Both the rechallenge and other group included 11 patients with ex-sensitive relapse (TFI ≥ 180 d). There was no significant difference in OS between the 2 groups (MST 15.7 vs. 26.9 mo, $P=0.46$).

Conclusions: Rechallenge chemotherapy did not prove superior to other chemotherapies, suggesting that monotherapy, such as amrubicin, might be reasonable as second-line chemotherapy for sensitive-relapse SCLC patients.

Key Words: small cell lung cancer, rechallenge chemotherapy, second-line, sensitive relapse, amrubicin

(*Am J Clin Oncol* 2013;00:000–000)

Lung cancer is the most common cause of cancer-related death. Small cell lung cancer (SCLC) accounts for approximately 12% of lung cancers.[1] SCLC has a very aggressive course, with approximately 60% to 70% of patients having disseminated disease at diagnosis. Although SCLC shows high sensitivity to chemotherapy and radiotherapy, about 80% of limited-disease patients and virtually all patients with extensive disease will develop disease relapse or progression.[2] The prognosis of relapsed SCLC patients is 2 to 4 months without treatment.[3]

Second-line chemotherapy may produce tumor regression, but the evidence of a clinical benefit is limited. In a phase III trial comparing oral topotecan with best supportive care, the median survival time (MST) was 25.9 weeks for patients receiving topotecan and 13.9 weeks for those receiving best supportive care (HR, 0.64; 95% CI, 0.45-0.90; $P=0.0104$).[4] Thus the efficacy of second-line chemotherapy for relapsed SCLC was demonstrated. However, selectable drugs are limited and topotecan is currently the only drug approved for the treatment of relapsed SCLC patients in the United States.[4–6]

Previous reports have shown that sensitive-relapse SCLC patients have a good chance of responding to the same induction chemotherapy (rechallenge chemotherapy).[7,8] Giaccone and colleagues reported the efficacy of rechallenge chemotherapy in 13 relapsed SCLC patients for whom the median treatment-free interval (TFI) was 30 weeks and the overall response rate (ORR) was 50%. Postmus and colleagues analyzed 37 relapsed SCLC patients and reported that the ORR of rechallenge chemotherapy was 62% (median TFI was 34 wk). Although these results suggest the effectiveness of rechallenge, the reported induction regimens were CAV (cyclophosphamide, doxorubicin, vincristine) or CDE (cyclophosphamide, doxorubicin, etoposide), which are not standard regimens at this time. It is unclear whether rechallenge with the currently standard regimens is effective. Therefore, to evaluate the efficacy of rechallenge with current induction regimens, we performed a retrospective analysis of second-line chemotherapy for sensitive-relapse SCLC patients.

MATERIALS AND METHODS

Patients

We collected data between September 2002 and May 2011 from the medical records of the Shizuoka Cancer Center. In this study, we defined TFI as the period from the date of completion of first-line treatment to the first relapse. When sequential radiotherapy or prophylactic cranial irradiation (PCI) was performed as first-line treatment, the date of completion of first-line treatment was defined as the last day of these treatments. We defined sensitive relapse as TFI ≥ 90 days, based on the definition in several previous trials.[9–11] Patients with TFI ≥ 180 days were considered as "ex-sensitive relapse," based on the NCCN guideline recommendation for rechallenge chemotherapy.

From the Divisions of *Thoracic Oncology; †Diagnostic Radiology; and ‡Pathology, Shizuoka Cancer Center Hospital, Nagaizumi-cho, Suntou-gun, Shizuoka, Japan.

Supported by the National Cancer Center Research and Development Fund 24-013 (N.Y.) and 24-008 (N.Y.).

The authors declare no conflicts of interest.

Reprints: Hirotsugu Kenmotsu, MD, Division of Thoracic Oncology, Shizuoka Cancer Center Hospital, 1007 Shimonagakubo, Nagaizumi-cho, Suntou-gun, Shizuoka 411-8777, Japan. E-mail: h.kenmotsu@scchr.jp.

ISSN: 0277-3732/13/000-000

DOI: 10.1097/COC.0b013e318286907b